



## Review

# A survey on synthesis of compliant constant force/torque mechanisms<sup>☆</sup>

Jie Ling<sup>a,\*</sup>, Tingting Ye<sup>b</sup>, Zhao Feng<sup>c</sup>, Yuchuan Zhu<sup>a</sup>, Yangmin Li<sup>d</sup>, Xiaohui Xiao<sup>b</sup>

<sup>a</sup> College of Mechanical and Electrical Engineering, Nanjing University of Aeronautics and Astronautics, Nanjing 210016, China

<sup>b</sup> School of Power and Mechanical Engineering, Wuhan University, Wuhan 430072, China

<sup>c</sup> Faculty of Science and Technology, University of Macau, 999078, Macao Special Administrative Region of China

<sup>d</sup> Industrial and Systems Engineering Department, The Hong Kong Polytechnic University, Hung Hom, Kowloon, 999077, Hong Kong Special Administrative Region of China



## ARTICLE INFO

## Keywords:

Constant force mechanism  
Compliant mechanism  
Synthesis method  
Structural optimization  
Kinetostatic modeling

## ABSTRACT

To avoid complicated force control system in precision manipulation, compliant constant force/torque mechanisms are proposed and developed continuously since the 1990s. The inherent nonlinearities due to varying stiffness raise high requirements for mechanism design, kinetostatic modeling and structural optimization. This makes the synthesis of compliant constant force/ torque mechanism a multidisciplinary and multiplex task. In this work, a comprehensive survey on synthesis methods of the constant force mechanisms is conducted. Three categories of synthesis methods are summarized, i.e., the Rigid-body Replacement approach, the Building Block approach and the Structural Optimization approach. For each category, the corresponding modeling and optimization methods are introduced in details. The presented survey provides overall perspectives on current status and future challenges in this field for designers and researchers.

## 1. Introduction

Extensive researches have shown that the synthesis of compliant mechanisms becomes a critical issue in the field of precision manipulation, such as precision engineering [1,2], biomedical engineering [3], energy harvesting [4] and so on. Typical applications of compliant mechanisms can be traced back thousands of years [5]. The aircraft invented by the Wright brothers initially used compliant mechanisms as warping wings [6]. However, it was not until the 1980s that the concept of “compliant mechanism” was clearly defined by Midha et al. The compliant mechanisms depend on the elastic deformation of their flexible segments to transfer force and displacement for the accomplishment of the specified operations [7]. In the literature [8], the compliant mechanisms are classified into lumped, distributed and hybrid types based on the size of their compliant areas. Compared to the rigid-body mechanisms, the compliant mechanisms are not only applied to fulfill the tasks without wear, backlash, friction and assembly but also integrated into micro-systems preferably on account of their miniaturized dimensions, which presents the unique merits in high precision manipulations [9–11]. Triggered by the scaling effect and contact hysteresis [12], the demands for high positioning and force precision need to be carefully addressed. As for the former, the survey by Sabarianand et al. [13] has shown that the researches

<sup>☆</sup> This document is the results of the research project funded by Natural Science Foundation of China [Grant No. 51375349], Natural Science Foundation of Jiangsu Province [Grant No. BK20210294], China Postdoctoral Science Foundation [Grant No. 2018M642905], and University of Macau under UM Macao Talent Programme [Grant No. UMMTP-2020-01].

\* Corresponding author.

E-mail addresses: [meejling@nuaa.edu.cn](mailto:meejling@nuaa.edu.cn) (J. Ling), [tilda\\_ye@whu.edu.cn](mailto:tilda_ye@whu.edu.cn) (T. Ye), [zhaofeng@um.edu.mo](mailto:zhaofeng@um.edu.mo) (Z. Feng), [meeyczhu@nuaa.edu.cn](mailto:meeyczhu@nuaa.edu.cn) (Y. Zhu), [yangmin.li@polyu.edu.hk](mailto:yangmin.li@polyu.edu.hk) (Y. Li), [xhxiao@whu.edu.cn](mailto:xhxiao@whu.edu.cn) (X. Xiao).

<https://doi.org/10.1016/j.mechmachtheory.2022.104970>

Received 2 April 2022; Received in revised form 31 May 2022; Accepted 31 May 2022

Available online 14 June 2022

0094-114X/© 2022 Elsevier Ltd. All rights reserved.

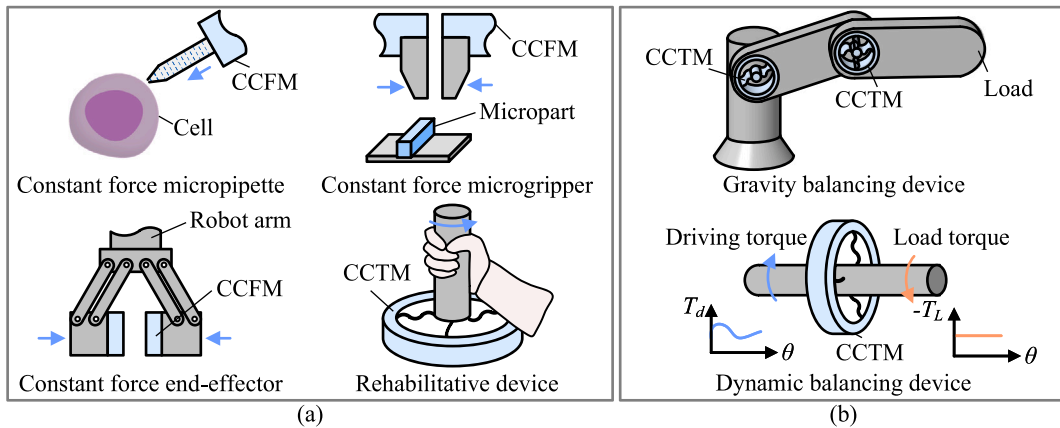


Fig. 1. Potential applications of compliant constant force/torque mechanism: (a) force limiting/assisting devices, and (b) gravity/dynamic balancing devices.

on positioning control theories and methods are relatively mature, especially in the piezo-actuated positioning systems [14–16]. As for the latter, one of the significant current discussions about appropriate contact force is whether to adopt control system [17] or design special compliant mechanism without force control requirements [18].

The contact force between the end-effector and the operating object in precise manipulation is often at sub-newton level [19–21], or even sub-millinewton level [22]. The sensing, calibration and modeling of the contact force are commonly realized by the force feedback technology based on precise sensory apparatus [23]. Therefore, a series of applications such as image processing technology, force modeling technology, data processing and transmission technology become the precondition of force control. Moreover, several force control algorithms have been proposed, including active stiffness control, impedance control, admittance control, explicit force control, implicit force control and so on [24,25]. Although the force control method often corresponds to the advantages of simple structure and good robustness, it has great limitations in the cost, complexity and technology integration of the control system. By contrast, a special kind of compliant mechanism, compliant constant force/torque mechanism (CCFTM), that can deliver a nearly constant output force/torque over a range of input displacement/angle is prone to reduce the complexity of various parts of the whole system, to relieve the signal processing burden, and to cut down the hardware and software costs [26].

### 1.1. Problem statement

Midha et al. [27] first proposed a compliant constant force mechanism (CCFM) based on kinematic limb-singularity of crank–slider linkage with springs, whose constant force could only reach tens of newtons with large fluctuation in a few centimeters after preloading more than ten centimeters, and was not yet qualified for precision manipulation. Similarly, Lan et al. [28] proposed a compliant constant torque mechanism (CCTM) based on structural optimization to compose a gripper in robot-assisted surgical manipulation. In order to broaden the application scenario, many efforts on the synthesis of compliant constant force/torque mechanisms (CCFTM) have been conducted in succession since then. Many potential applications can be reflected in the following aspects:

- **Force limiting/assisting device.** As shown in Fig. 1(a), the CCFTMs can be adopted as the end-effectors by limiting the output force/torque in a proper range in applications where the operating objects need to avoid overload damage, such as constant force micropipette in microinjection [29], the constant force microgripper in micro assembly [30], and the end-effector in robotic system [31]. On the other hand, they can also serve as rehabilitative devices, fitness equipment, haptic devices and braille cells by providing mobility assistance or maintaining constant training force/torque [32,33].
- **Gravity/dynamic balancing device.** As shown in Fig. 1(b), the CCFTMs can be used for gravity balancing in the robotic system to minimize the input torques [34], which has better compactness than their rigid-body counterparts with multiple springs. They can also serve as static balancing device, combining the merits of compliant mechanisms and rigid mechanisms, i.e., high precision and zero energy storage [35]. Besides, they can also achieve dynamic balancing in the electromechanical system by converting the fluctuating input torque to the constant output torque, thus contributing to the minimization of fluctuation of output speed [33,36].

Synthesis is the process from functional demand to achieve the expected goal. As far as specific applications are concerned, the synthesis procedure of generating CCFTMS can be divided into several levels: functional demands, principle design, method selection, virtual prototyping and physical prototyping, as shown in Fig. 2.

- **Functional requirement.** According to a specific application, the required functions can be analyzed and proposed, such as kinetostatic performance, dynamic performance, fatigue performance and so on. Among them, the kinetostatic performance is the most critical and interesting factor, which refers to the relation between the force/torque and displacement, including the

Applications	Force limiting/assisting devices	Static/dynamic balancing devices
Functional demands	<ul style="list-style-type: none"> <li><b>Kinestatic performance</b> <ul style="list-style-type: none"> <li>Constant force/torque value <math>F_c/T_c</math></li> <li>Constant force/torque stroke <math>d_c/\theta_c</math></li> <li>Constant force/torque fluctuation <math>F_f/T_f</math></li> <li>Constant force stage <math>n</math></li> <li>Preload stroke <math>d_p/\theta_p</math></li> <li>Degree-of-freedom</li> </ul> </li> <li><b>Other performances</b> <ul style="list-style-type: none"> <li>Dynamic performance</li> <li>Fatigue performance</li> </ul> </li> </ul>	<p>Force(Torque)-Displacement(angle) Curve</p>
Conceptual design	<ul style="list-style-type: none"> <li><b>Principle design</b> <ul style="list-style-type: none"> <li>Kinematic limb-singularity</li> <li>Topological optimization</li> </ul> </li> <li><b>Configuration design</b> <ul style="list-style-type: none"> <li>Stiffness combination configuration</li> </ul> </li> </ul>	<ul style="list-style-type: none"> <li>Beam buckling theory</li> <li>Direct zero stiffness configuration</li> </ul>
Approach selection	<ul style="list-style-type: none"> <li><b>Synthesis approaches</b> <ul style="list-style-type: none"> <li>Rigid-body Replacement approach</li> <li>Building Block approach</li> </ul> </li> </ul>	<ul style="list-style-type: none"> <li>Topological Optimization approach</li> <li>Freedom and Constraint Topology approach</li> </ul>
Virtual prototyping	<ul style="list-style-type: none"> <li><b>Kinestatic modeling method</b> <ul style="list-style-type: none"> <li>Pseudo rigid-body method</li> <li>Elliptic Integral method</li> <li>Chained Beam Constraint method</li> </ul> </li> <li><b>Optimization algorithm</b> <ul style="list-style-type: none"> <li>Gradient-based algorithm</li> </ul> </li> </ul>	<ul style="list-style-type: none"> <li>Shooting method</li> <li>Finite Element Analysis software</li> <li>Heuristic algorithm</li> </ul>
Physical prototyping	<ul style="list-style-type: none"> <li><b>Additive manufacturing</b></li> </ul> <p>CCFM<sup>[37,38]</sup></p>	<ul style="list-style-type: none"> <li><b>Traditional manufacturing</b></li> </ul> <p>CCTM<sup>[39,33]</sup></p>

Fig. 2. Synthesis procedure of compliant constant force/torque mechanisms [33,37–39] (Reprinted from Pham and Wang [37] (Copyright 2011 by Elsevier); Reprinted from Chen and Lan [38] (Copyright 2012 by Elsevier); Reprinted from Li and Hao [39] (Open Access); Reprinted from Hou and Lan [33] (Copyright 2012 by Elsevier).

constant force/torque value  $F_c/T_c$ , the constant force/torque stroke  $d_c/\theta_c$ , the constant force/torque fluctuation  $F_f/T_f$ , the constant force stage  $n$ , the preload stroke  $d_p/\theta_p$ , and the degrees-of-freedom. For instance, the micro assembly of polarization maintaining optical fiber requires two kinematic degree-of-freedom CCFMs [40]; the micro assembly of micro parts with multiple sizes can achieve better operation and protection effect by using multi-stage CCFMs [41]; the eradication of the preloading stroke can avoid weakening the constant force performance of CCTMs, which often occupies more than one-third of the whole stroke [42,43].

- **Conceptual design.** The principle to generate CCFTMs is to store and release energy through the deformation of compliant joints, and keep the component force/torque constant in a certain direction by combining with the rigid segment. The design principles can be classified into three categories, including the kinematic limb-singularity, the beam buckling effect, and the topology optimization, which will be introduced in detail in subsequent sections. On this basis, two type configurations are main concerns, including stiffness combination configuration [44–49] and direct zero stiffness configuration [48,49] (refer to Section 2.2.2).
- **Approach selection.** The synthesis approaches of compliant mechanisms have been systematically and comprehensively reviewed and introduced before, including the rigid-body replacement approach (RBRA), the building block approach (BBA), the topological optimization approach (TOA), and the freedom and constraint topology based approach [7,50–52]. RBRA is

a commonly used method, which usually replaces the kinematic pairs of a rigid-body constant force/torque mechanism that can achieve the expected task with flexible joints. BBA combines standard components that can provide specific functions, such as the horizontal homogeneous straight beam as a positive stiffness component and the inclined homogeneous straight beam as a negative stiffness component. It should be noted that a mechanism shows the positive stiffness when the stored energy increase with the increase of the deformation, while the negative stiffness appears with the decrease in energy [41]. Herein, if a negative stiffness mechanism is connected with a positive stiffness mechanism, the zero-stiffness mechanism will be derived. TOA achieves the desired goal by topology optimization in the design domain or multi-parameter optimization of beams with explicit shape functions. Since the main object of this review is the basic element that can realize constant force, where the kinetostatic performance is major concerned, little attention needs to be paid to the freedom and constraint topology based approach which uses flexible joints to constrain rigid bodies to produce the desired degrees of freedom [7], where the kinematic performance is major concerned. The detailed comparisons of the above three methods (i.e., RBRA, BBA and TOA) will be discussed in Section 4.

- **Virtual prototyping.** After the principle and configuration of a CCFTM are determined, it is necessary to conduct virtual prototyping for kinetostatic (constant force) performance to obtain the theoretical modeling results, which is convenient for subsequent configuration adjustment or parameter optimization. As to the kinetostatic modeling method, the pseudo-rigid-body method based on the virtual work principle is usually used in RBRA; the Elliptic Integral method based on the Euler–Bernoulli beam theory and the Chained Beam Constraint method based on the Timoshenko beam theory are widely applied in BBA; the Shooting method based on the Euler–Bernoulli beam theory, and the Finite Element Analysis (FEA) software are all employed in TOA.
- **Physical prototyping.** The common ways for physical prototyping of CCFTMs contain traditional manufacturing and additive manufacturing. As to the traditional manufacturing, the wire electrical discharge machining with aluminum alloy, spring steel, and stainless steel is the most widely used method in CCFTMs with standard compliant joints, which are basically synthesized by RBRA and BBA. As to the additive manufacturing, its application scope covers almost all types of CCFTMs. Especially for CCFTMs synthesized by TOA with nonstandard shapes of compliant joints, the additive manufacturing endows them with much better machinability than the traditional manufacturing. Frequently seen additive manufacturing materials for CCFTMs include Polyoxymethylene [31], electroplated nickel [53], engineering plastic [54] and so on.

### 1.2. Motivation

It is apparent that the synthesis methods of CCFTMs have the characteristics of many contents and strong intersection without a mature theoretical system. So far, there are some published review papers related to CCFTMs [18,55], but there seems exist the following limitations.

- Firstly, the published reviews are not comprehensive enough and classified clearly for the types of CCFTMs, mainly focusing on a single aspect or a single method in synthesis of CCFTMs. Especially for the synthesis methods of multi-stage CCFTMs, the survey work cannot be found as far as the authors' knowledge.
- Secondly, there are still some deficiencies in the comparative studies and practical guidelines of synthesis methods from an overall perspective. Without intuitive comparisons and straightforward guidance, it is difficult for beginners to directly choose fast and accurate modeling methods and tools.
- Lastly, lacking the summary of rigid-body replacement ways and the establishment of building block library, the application of RBRA and BBA needs a lot of preliminary investigations and method attempts, which greatly weakens their advantages of simplicity and ease of usage.

The comparisons between featured surveys and this work are briefly listed in Table 1. However, it should be noted that the soft-body compliant mechanism based on soft materials is not the emphasis of this survey.

### 1.3. Contributions

In order to enable interested researchers to quickly and comprehensively understand the synthesis of CCFTMs, this survey reports the recent research advances. The main contributions of this survey are as follows:

- A comprehensive overview of the proposed CCFTMs so far including synthesis methods and a clear classification based on the design principles (i.e., kinematic limb-singularity, beam buckling theory and topological optimization) are presented for readers.
- Comparative studies and practical guidelines of the synthesis methods (RBRA, BBA, TOA) based on the above three types of CCFTMs as well as their kinetostatic modeling methods (Elliptic Integral method [41], Chained Beam Constraint method [11] and FEA) are provided for design references.
- Establishment of the replacement ways of RBRA, the building block library of BBA, and the geometries of CCFTMs of TOA are discussed.
- The future development trend of CCFTMs is also discussed, which provides some direction suggestions for practitioners to synthesize CCFTMs with better performances and develop more advanced synthesis methods.

**Table 1**  
Comparisons between featured surveys in the literature and this survey.

Surveys	Authors	Topic	Description	Year
[55]	Weight, B. L.	Design and modeling method	It mainly reviews the CCFMs based on crank–slider mechanism in the 1990s, and introduces the pseudo rigid-body method.	2002
[18]	Wang, P. and Xu, Q.	Design and modeling method	The CCFMs proposed before 2018 are classified according to mechanism features, and some classic modeling methods are introduced.	2018
This survey	Ling, J. et al	Synthesis methods	The CCFMs proposed before 2022 are overviewed and classified by the synthesis methods, including design, modeling and optimization, and the adopted modeling and optimization methods are summarized comprehensively.	2022

#### 1.4. Organization

The remainder of this survey is organized as follows. The classifications of the existing and possible configurations are summarized in Section 2. The comparisons of constant force performances are conducted in Section 3. The comparative studies of employed synthesis approaches are carried out in Section 4, including the kinetostatic modeling methods, the topological optimization methods and optimization algorithm. Section 5 discusses the merits, shortages and application fields of synthesis approaches. Finally, the challenges and future trends are concluded in Section 6 .

## 2. Conceptual design of compliant constant force/torque mechanisms

### 2.1. Classification of compliant mechanisms

In terms with mechanism type, the compliant mechanisms can be classified into the partial compliant mechanism and the fully compliant mechanism, as shown in Fig. 3(a). Compared with the partial compliant mechanism, the fully compliant mechanism has the characteristics of higher precision and smaller stroke because it only depends on the deformation of the flexible segments to transfer motion and force, presenting better practicability in precision manipulations, including microinjection, micro assembly, micro machining, etc. On the other hand, the partial compliant mechanisms has much larger motion strokes than the fully ones, which can be widely used in robotics and rehabilitation medicine. In addition, the compliant mechanisms have relatively low payload ability and small motion range than the rigid ones. At the element level, the flexible segments can be divided into the short length flexure hinges and the long length flexure beams based on the size of their compliant areas. The short length flexure hinges generally include the round notch hinge, the elliptical notch hinge, the short armed notch hinge, the cross reed flexure hinge, and the wheel type flexure hinge, as shown in Fig. 3(b). In addition, some flexure hinges with irregular shapes based on topological optimization can achieve the optimal material distribution aiming at the specified objectives [56,57]. The long length flexure beams can be further divided into two categories, i.e., the standard type and nonstandard type (see Fig. 3(c)). The central axis of the standard flexure beam is a straight line, whose sections are homogeneous. On the contrary, the nonstandard flexure beams contain the straight beam with inhomogeneous sections, the curved beam with homogeneous sections, and the curved beam with inhomogeneous section.

### 2.2. Compliant constant force/torque mechanisms based on kinematic limb-singularity

#### 2.2.1. Kinematic limb-singularity

The kinematic limb-singularity is a common property of rigid-body linkages, which is usually adopted to construct the kinetostatic nonlinear stiffness characteristic [39,58]. Inspired by the kinematic limb-singularity of the mechanisms with springs [59], their intrinsic nonlinear kinetostatic performances give them the potential to be applied to the synthesis of CCFTMs. As shown in Fig. 4(a), the mechanisms with springs that have been used for CCFMs include the crank–slider mechanism [49] and the double slider mechanism [58]. As shown in Fig. 4(b), the mechanism with springs that has been used for CCTMs mainly is the crank–slider mechanism [39].

Since the crank–slider mechanism is most frequently used in synthesizing CCFTMs based on kinematic limb-singularity, the following takes it as an example of CCTM to further explain the design principle. Singular position is a kind of special position in the mechanism with springs, where the motion of the mechanism is unstable. As shown in Fig. 4(c), the crank–slider mechanism reaches its singular positions once the crank  $AB$  and the rod  $BC$  are in a straight line. Obviously, the crank–slider mechanism has two singular positions. In practical terms, only the singular position where joint  $B$  is between joint  $A$  and joint  $C$  is generally

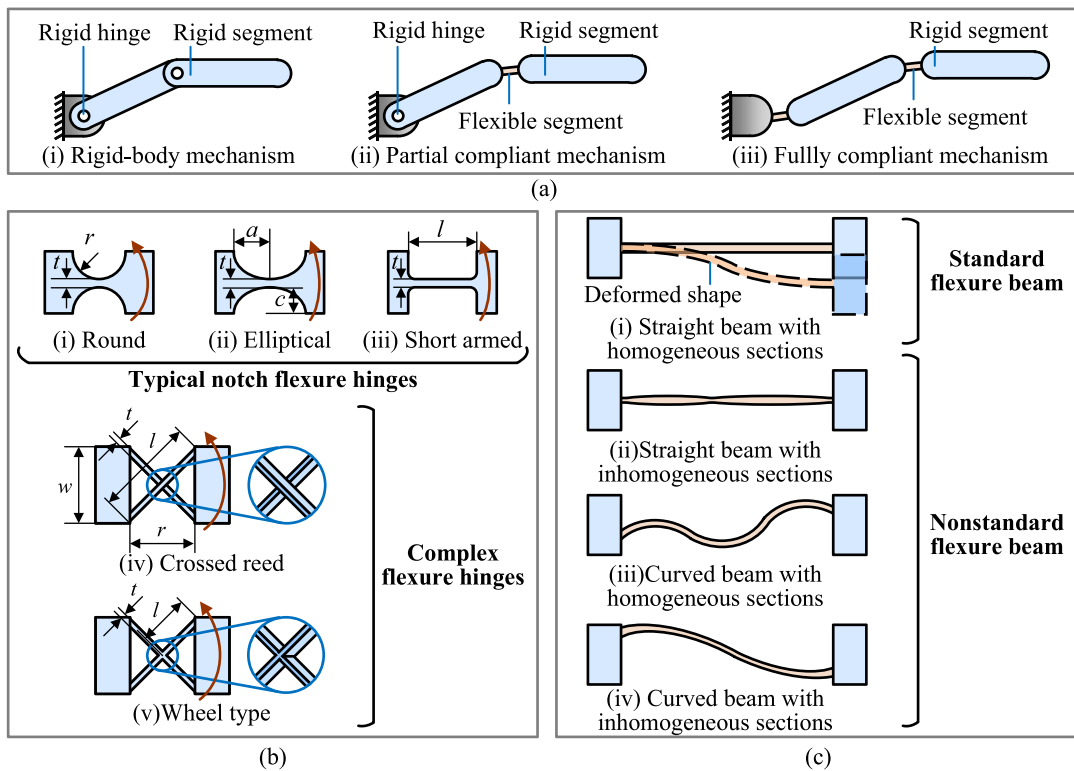


Fig. 3. Comparison of compliant mechanisms at the mechanism and element level: (a) conceptual comparison of rigid-body mechanism, partial compliant mechanism and fully compliant mechanism, (b) exemplary short length flexure hinges, and (c) exemplary long length flexure beams.

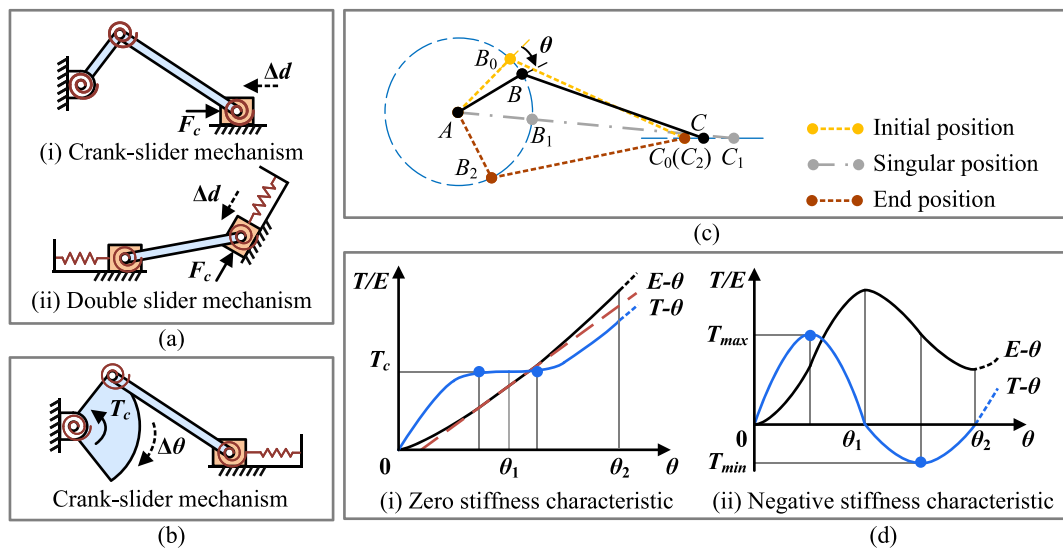


Fig. 4. Illustration of kinematic limb-singularity of the mechanisms with springs: (a) configurations of CCFMs based on kinematic limb-singularity, (b) configurations of CCTMs based on kinematic limb-singularity, (c) singular position of crank-slider mechanism, and (d) nonlinear kinetostatic performances of crank-slider mechanism.

adopted due to the yield strength limitation of flexible joints. When the crank  $AB$  moves from the non-singular initial position  $A_0B_0$  to the singular position  $A_1B_1$ , the elastic potential energies of torsion springs increase accordingly, so does the linear spring's. When the crank  $AB$  moves from the singular position  $A_1B_1$  to the non-singular end position  $A_2B_2$ , the elastic potential energies of torsion



springs still increase accordingly, while those of linear spring are on the contrary. The motion output of the mechanism is uncertain when the mechanism is in a singular position, which is a double-edged sword [60]. On the one hand, the velocity of the follower at the singular position is close to zero, which will make the mechanism immobilized. Thus, a few studies of the singularity analysis and avoidance are implemented [61]. On the other hand, the nonlinear stiffness produced by the process of energy storage and release can help to construct a CCFTM [62].

According to the Hooke's law, the force–displacement curve is approximately a straight line before yielding. Therefore, the linear stiffness of spring and torsional stiffness of each rigid joint can be approximately regarded as constant values. With the well-designed stiffness of the torsion springs and linear spring in the crank–slider mechanism, it can show nonlinear kinetostatic performances, such as local zero stiffness characteristic and negative stiffness characteristic (see Fig. 4(d)). Some related researches [39,58] indicate that the above two situations are possible only the stiffness of the linear spring is not zero. In addition, when the stiffness of linear spring is constant, sufficiently small stiffness of torsional springs may produce nonlinear negative stiffness of the crank–slider mechanism, and sufficiently large stiffness of torsional springs may produce nonlinear positive stiffness of the crank–slider mechanism. Therefore, the constant force performance of the crank–slider mechanism can be obtained with the well-designed parameters of the torsion springs and the linear spring.

### 2.2.2. Classification of configurations

The existing configurations of CCFTMs based on kinematic limb-singularity generally contain two types, i.e., stiffness combination configuration and direct zero stiffness configuration. Among them, the standard flexure beam and nonstandard flexure beam have been defined in Section 2.1. Murphy et al. [27] proposed and summarized 28 configurations of CCFMs based on crank–slider mechanism, which are classified according to their number of flexure segments. Then, Weight [55] refined the classification and developed a new nomenclature in the light of the types of compliant and rigid segments, as shown in Fig. 5(a). To be specific, the letter “s” refers to the short length flexure hinge; the letter “l” refers to the long length flexure beam; the “p” refers to the rigid pivot (see Fig. 5(a)).

On this basis, the viable configurations of CCFTMs based on kinematic limb-singularity are listed and classified in Fig. 5. For ease of expression, the CCFTMs using kinematic limb-singularity generated by the combination of positive and negative stiffness mechanisms are classified as Class KA; the CCFTMs generated by the optimized direct zero stiffness mechanism are classified as Class KB. The viable configurations of CCFMs based on crank–slider mechanism are shown in Fig. 5(b). The Class KA CCFMs are further classified by the number and arrangements of those flexible segments. The subclasses of the Class KA CCFMs are determined by the number of the constant force stages, and the configurations of ones are nominated by the arrangements of those flexible and rigid segments. For example, a Class KA-1-*spp* has one short length flexure hinge located at the first pivot from left to right; a Class KA-1-*spl* has two flexible segments, in which the short length flexure hinge is arranged at the first pivot, and the long length flexure beam is arranged at the last pivot from left to right. The existing Class KA CCFMs based on crank–slider mechanism mainly contain Class KA-1-*ppl* [44,45], Class KA-1-*plp'* [46], Class KA-1-*lpl* [47], and Class KA-1-*sss* [63,64]. Besides, a Class KB configuration based on crank–slider mechanism is proposed by Bilancia et al. [48,49], which is inspired by the Class KA-1-*sss* configuration and composed of a nonstandard straight flexure beam with inhomogeneous sections.

Similarly, the viable configurations of CCFMs based on double slider mechanism are proposed, listed and classified as shown in Fig. 5(c). Different from the crank–slider mechanism in the preceding paragraph, the double slider mechanism has a spring slider part additionally, which is nominated as guided mechanism. The common configurations and letters of the guided mechanisms can be seen in Fig. 5(d). For example, a Class KA-1-*gcsp* has a *gc* type guided mechanism, which is connected with a short length flexure hinge. The existing CCFMs based on double slider mechanism include Class KA-1-*gcss* [65] and Class KA-1-*gdss* [58]. It is worth mentioning that the symmetrical arrangement is frequently used in CCFMs based on kinematic limb-singularity to obtain the guiding effect of input displacement.

As to the viable configurations of CCTMs based on crank–slider mechanism, the specific information will not be expanded, since the configurations of crank–slider mechanism and guided mechanism have been introduced in detail above. The existing CCTM based on crank–slider mechanism belong to Class KA-1-*sslgc* [39].

## 2.3. Compliant constant force/torque mechanisms based on beam buckling theory

### 2.3.1. Beam buckling theory

In the engineering field, when the structure is subjected to axial pressure, the buckling deformation is prone to occur, which reduces the lateral bearing capacity, and even lead to serious accidents, such as in bridges [66]. Inspired of that, the flexure beams based on beam buckling theory are widely used for synthesis of CCFTMs due to their nonlinear kinetostatic performance, i.e., negative stiffness characteristic. The typical bi-stable flexure beam can be seen in Fig. 6, which is composed of inclined straight beams with homogeneous sections. Taking this as an example, the principle of its stiffness characteristic will be briefly introduced below.

The deformation shapes of the beam as well as the changes of strain energy and stiffness performance are described as follows:

- The initial undeformed shape  $d = 0$  is a straight line  $\overline{O_F O}$  with a inclined angle to the fixed end. The strain energy is 0.
- The positive stiffness is expressed before the first critical buckling position  $d \in (0, d_1)$ , and the deformed curve is denoted as  $\overline{O_F A}$  with one inflection point. The maximum reaction force  $F_{max}$  shows when the displacement reaches the first critical buckling position  $d_1$ . During this period, the strain energy increases with growing speed.

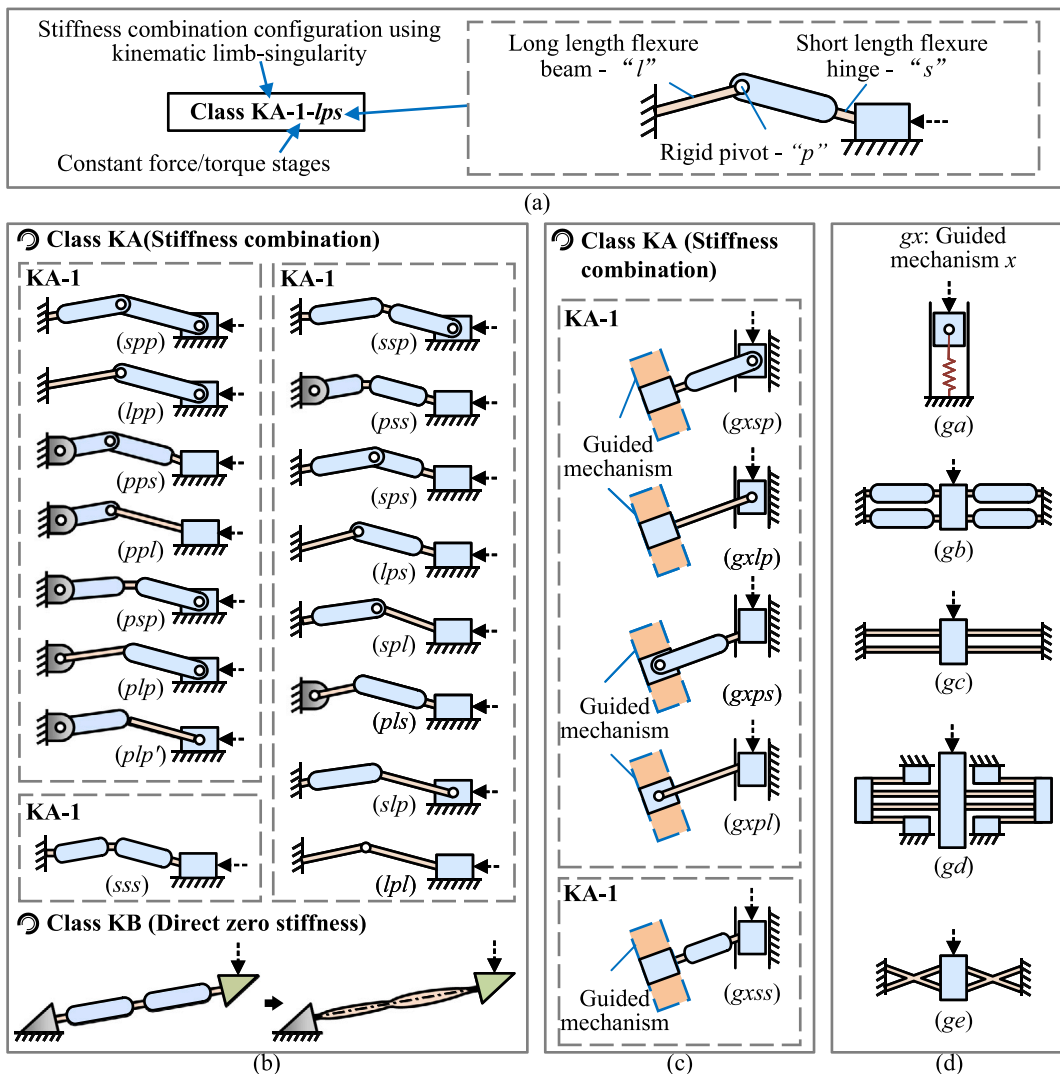


Fig. 5. Viable configurations and classification of compliant constant force mechanisms based on kinematic limb-singularity: (a) meaning of abbreviation letters, (b) viable configurations of compliant constant force mechanisms based on crank-slider mechanism, (c) viable configurations of compliant constant force mechanisms based on double slider mechanism, and (d) viable configurations of guided mechanisms.

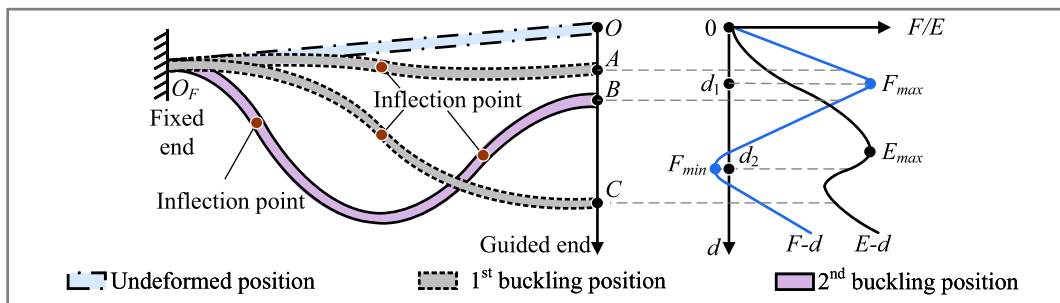


Fig. 6. Illustration of beam buckling theory.

- The negative stiffness appears between the two critical buckling positions  $d \in (d_1, d_2)$ , and the deformed curve is as  $\widehat{O_F B}$  with two inflection points. The minimum reaction force  $F_{min}$  shows when the displacement reaches the second critical buckling position  $d_2$ . The strain energy firstly increases with reducing speed, and then decreases with reducing speed.



- The positive stiffness is shown after the second critical buckling positions  $d \in (d_2, d_{yield})$ , and the deformed curve is as  $\widehat{O}_F C$  with one inflection point. The strain energy firstly decreases with growing speed, and then increases with growing speed.

### 2.3.2. Classification of configurations

The existing configurations of CCFMs based on beam buckling theory generally basically pertain to the stiffness combination configuration, which is nominated as Class BA for easy expression. Fig. 7 summarizes the viable configurations and classification of Class BA CCFMs, which are generated by the combination of positive and negative stiffness mechanisms. The pre-existing positive and negative stiffness mechanisms are shown in Fig. 8(a) and (b), respectively. The subclasses of the Class BA CCFMs are determined by the number of their constant force stages, and the configurations are nominated by the combination ways of the positive and negative stiffness mechanisms. To be specific, the letter “ $px$ ” refers to the positive stiffness mechanism; the letter “ $nx$ ” refers to the negative stiffness mechanism; the letter “ $/$ ” refers to the parallel combination; the letter “ $+$ ” refers to the series combination.

As shown in Fig. 7, the 1-stage CCFM is denoted as a CCFM with one segment of zero stiffness in the force–deformation diagram. Similarly, a CCFM with two segments of zero stiffness in the force–deformation diagram is denoted as a 2-stage CCFM. For the multi-stage CCFM, the multi segments of zero stiffness can be obtained either by combination of negative and positive stiffness beams or by adjusting the beam positions.

As to the CCFM that belongs to Class BA-1, the 1-stage constant force is realized by the parallel combination of the quasi-linear positive stiffness mechanism and 1-stage negative stiffness mechanism, i.e.  $px//nx$ . On this basis, many configurations have been developed, including Class BA-1- $pa//na$  [67–70], Class BA-1- $pb//na$  [71], Class BA-1- $pc//na$  [29,40,72–74]. Among them, Class BA-1- $pa//na$  is the simplest configuration. In practice,  $pa$  type flexure beam needs a longer length to fit with  $na$  type flexure beam [67–69], which is not conducive to structure miniaturization and brings some trouble to the traditional manufacturing. In addition, the stress stiffening effect caused by the axial tensile stress of  $pa$  type flexure beam will cause the positive stiffness to be nonlinear slightly. The comparative study between  $pa$ ,  $pb$  and  $pd$  type flexure beams has been conducted in [71], whose result shows that the  $pb$  and  $pd$  type flexure beams have better linearity than the  $pa$  type one. The  $pb$  beam can reduce the stress stiffening effect by the torsional deformation of the middle vertical segment. For similar reasons, the  $pc$  type flexure beam not only has better stiffness linearity, but also can increase the effective length without changing the distance between the fixed end and the guided end. The above two types can reduce the stress stiffening effect, while the  $pd$  type structure can completely eliminate it. Composed of two symmetrical inclined straight beams,  $pd$  type structure has only torsional deformation on the beams without any axial tensile deformation. The  $pe$  type flexure beam is widely applied in the situation that require a pure translational motion [75].

As to the CCFM that belongs to Class BA-2, the 2-stage constant force is generally realized by the parallel combination of a linear positive stiffness mechanism and a 2-stage negative stiffness mechanism. The second stage constant force can be larger or lower than the first one. The key problem lies in the generation of the 2-stage negative stiffness mechanism, which can be achieved by the parallel or serial combination of two 1-stage negative stiffness mechanisms. Three viable configurations are listed in Fig. 7, including  $px//nx_1//nx_2$ ,  $px//(nx_1 + nx_2)$  and  $px//(nx_1 + nx_2)'$ . The force versus displacement ( $F - d$ ) curves of those 2-stage negative stiffness mechanisms in parallel and serial combination and the corresponding 2-stage constant force mechanisms are also given. As can be seen, the deformations of the  $nx_1$  and  $nx_2$  type negative stiffness mechanisms in parallel combination are synchronized, which means that the  $F - d$  curve of the  $nx_1//nx_2$  type 2-stage negative stiffness mechanism can be obtained by summing their  $F - d$  curves. Unlike this, the deformations of the  $nx_1$  and  $nx_2$  type negative stiffness mechanisms in serial combination are not simultaneous [76]. When one of them (e.g.  $nx_1$ ) undergoes the deformation in the process of “undeformed  $\rightarrow$  1<sup>st</sup>  $\rightarrow$  2<sup>nd</sup>  $\rightarrow$  1<sup>st</sup>” buckling modes, little deformation of the other one (e.g.  $nx_2$ ) occurs. After that, the  $nx_2$  type negative stiffness mechanism starts to deform, while the  $nx_1$  type negative stiffness mechanism is hardly deformed. Due to structural limitations, the  $nb$  type flexure beam is generally applied in the  $px//(nx_1 + nx_2)'$  type configuration, but rarely in other configurations. The proposed configurations of CCFMs that belong to Class BA-2 contain Class BA-2- $pa//na//na$  [41] and Class BA-2- $pe//(nb + na)'$  [71].

As to the CCFM that belongs to Class BA-m, the multi-stage constant force basically depends on an adjustable positive stiffness mechanism with some equipment, such as adjustment screw with stepper motor, hand tuning micrometer, and so on. Because the positive stiffness mechanisms need to be adjustable, the flexure beams that are similar to the fixed-guided beam have poor adaptability, such as  $pa$ ,  $pb$ ,  $pc$  and  $pe$  type ones. In contrast, the  $pd$  and  $pf$  type beams are more practical. The proposed configuration is Class BA-m- $(pd//na)'$  [77]. Although the adaptability of the contact force has been greatly increased by the use of adjustable devices, the Class BA-m configuration often suffers from poor continuity in varying the constant force, large space occupancy, and additional hardware and software requirements.

A part of configurations of CCTMs using beam buckling theory adopt  $na$  type flexure beams [42,78,79]. Especially, Gandhi et al. [42] proposed a CCTM using precompressed  $na$  type flexure, which completely eliminates the preload stroke  $\theta_p$ , maintaining the constant torque from 0 to 60°. Besides, Morsch et al. [80] proposed a cross reed type CCTM composed of two  $na$  type flexure beams, whose constant torque is realized by the combination of positive and negative stiffness mechanisms. In other words, the tension beam shows positive stiffness and the compression beam shows negative stiffness in the process of two flexure beams rotating around the intersection.

### 2.4. Compliant constant force/torque mechanisms based on topological optimization

Topology denotes the distribution of solid materials and voids in the design domain. For the known optimization objectives, the topological optimization realizes the optimal configuration of finite materials in a specific design area under known constraints [84]. Recently, Zhu et al. [85] conduct a review of the synthesis of compliant mechanisms using continuum topological optimization,

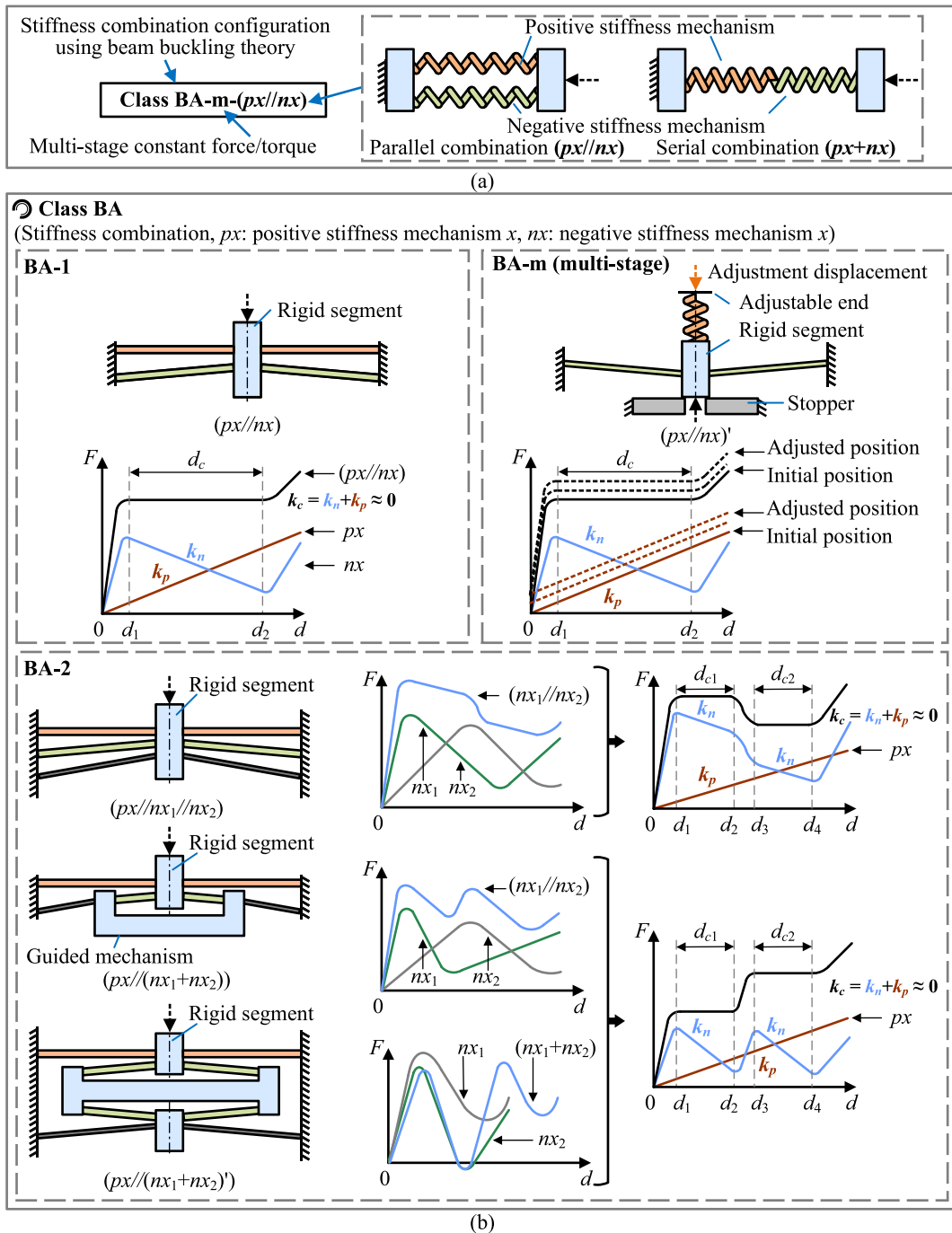


Fig. 7. Viable configurations and classification of compliant constant force mechanisms using beam buckling theory: (a) meaning of abbreviation letters, and (b) viable configurations.

where the categories of mathematical representations are presented, including the grid representation and the geometric representation. As shown in Fig. 9(a), with known objectives and constraints, the variables in grid representation are the finite elements generated by separating the design domain into the finite parts, where an element may be a solid (black) or a cavity (white); the variables in geometry representation are the properties of these parametric curved beams, such as the positions and numbers of control points, thickness, shape functions, etc.

To simplify expression, the stiffness combination configurations of CCFTMs using topological optimization are called Class TA; the direct zero stiffness configurations of CCFTMs using topological optimization are called Class TB. As to the CCFTMs using topological

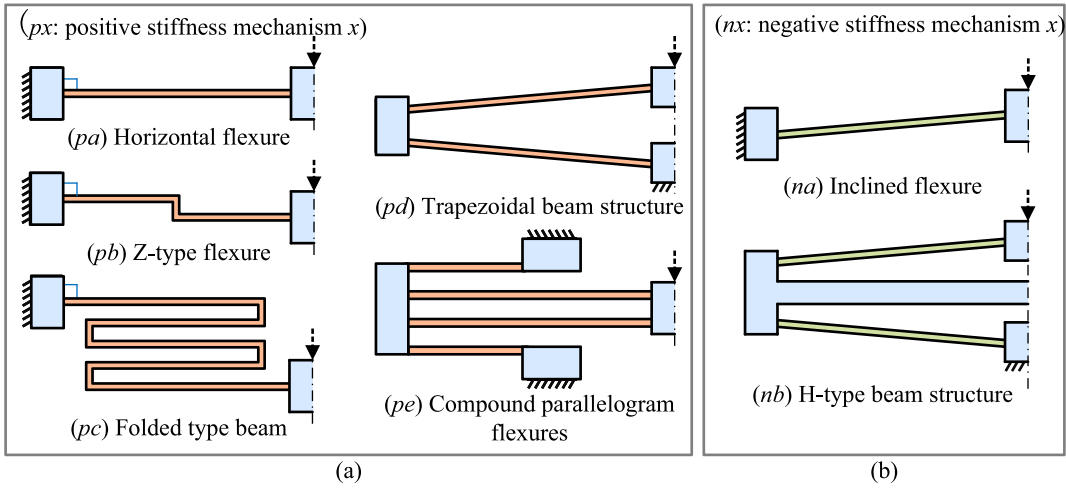


Fig. 8. Existing positive and negative stiffness mechanisms in compliant constant force mechanisms using beam buckling theory: (a) positive stiffness mechanisms and (b) negative stiffness mechanisms.

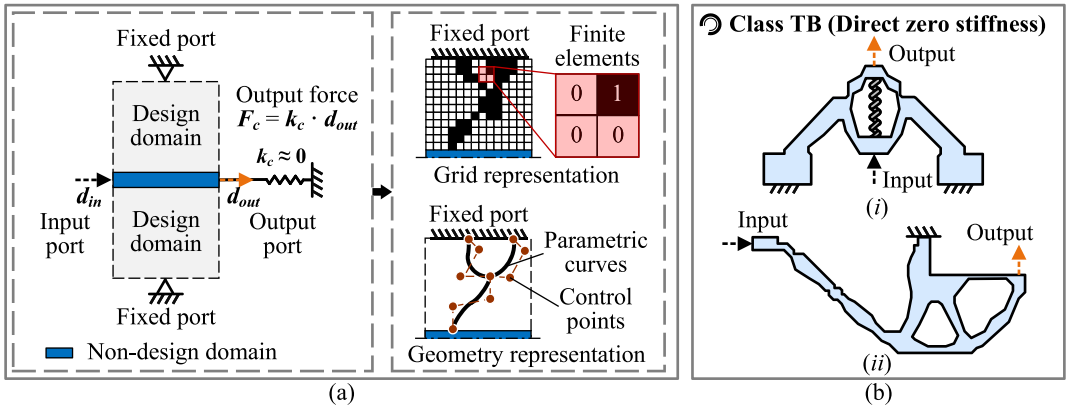


Fig. 9. (a) Illustration of topological optimization, and (b) Proposed compliant constant force mechanisms using topological optimization with grid representation, reproduced from [81–83].

optimization with grid representation, Liu et al. [81–83] developed two CCFMs for end-effectors in robotics, Class TB-*i* and Class TB-*ii*, as shown in Fig. 9(b). As to the CCFMs using topological optimization with geometric representation, many configurations have been proposed, as shown in Fig. 10. The letters of Class TA CCFMs are kept the same as Class BA ones mentioned before. As shown in Fig. 10(a), the raised configurations of Class TA CCFMs contain Class TA-*m*-(*pf*//*nc*)<sup>*t*</sup> [86]. In addition, although there are few applications so far, some negative stiffness mechanisms with nonstandard flexures show some potential for stiffness combination due to their superior linearity in large strokes, such as *nd* [90], *ne* [76,95], *nf* [88,89] and *ng* [91] type negative stiffness mechanisms. Among them, Wang et al. [76] proposed a (*ne* + *ne*) 2-stage negative stiffness mechanism, which is realized by the serial combination of two *ne* type negative stiffness beams. The proposed configurations of Class TB CCFMs include Class TB-*za* - TB-*zg* [30,31,37,53,87,92], in which the flexure beams are all homogeneous. As shown in Fig. 10(b), the existing configurations of CCTMs include Class TB-*zh* - TB-*zk* [28,33,54,93,94]. Among them, the flexure beam in Class TB-*zk* CCTM [54,93] is composed of two-segment Bezier curved inhomogeneous beams. Some curved beams with shape functions can be parameterized for programming, which brings great convenience to shape optimization and parameter optimization, such as the polynomial curves, Bezier curves and cosine curves. According to Fig. 11, the shape functions of those curved beams are represented as follows:

- **Polynomial curve.** The rotation angle  $\eta$  of  $m$ -order polynomial along the non-dimensional arc length  $u$  ( $u \in [0, 1]$ ) is as:  $\eta = c_0 + c_1u + \dots + c_mu^m$ .
- **Bezier curve.** The coordinates  $x$  and  $y$  of  $m$ -th order Bezier curve along the non-dimensional arc length  $t$  ( $t \in [0, 1]$ ) are as:  $x = \sum_{i=0}^{m-1} Q_{ix}B_i$ ,  $y = \sum_{i=0}^{m-1} Q_{iy}B_i$ , where the Bernstein polynomial  $B_i = \frac{(m-1)!}{(i!(m-1-i)!)} \cdot t^i(1-t)^{m-1-i}$ ;  $Q_{xi}$  and  $Q_{yi}$  are the  $x$  and  $y$  coordinates of control point  $Q_i$ .

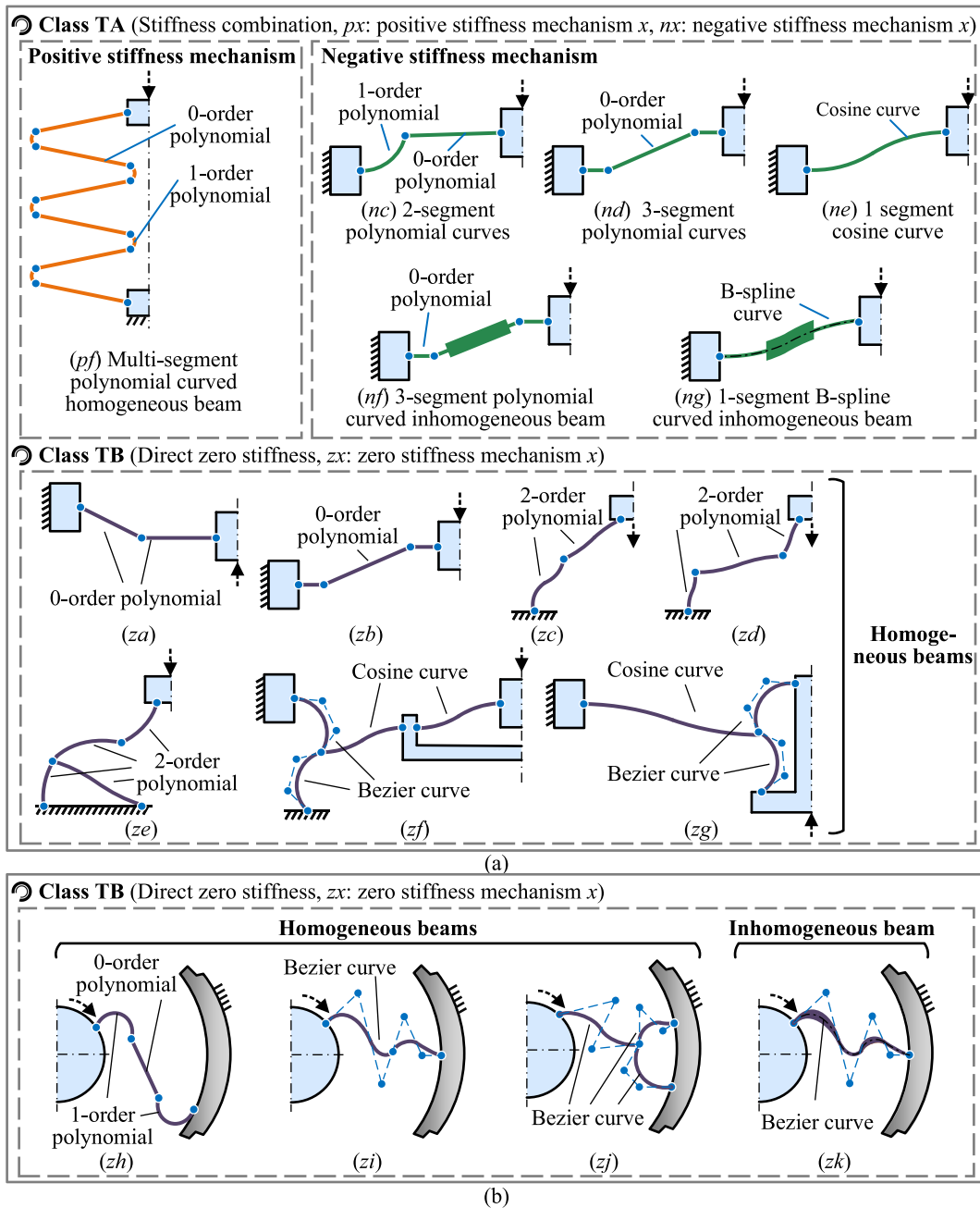


Fig. 10. Proposed compliant constant force/torque mechanisms using topological optimization with geometry representation: (a) existing configurations of compliant constant force mechanisms, and (b) existing configurations of compliant constant torque mechanisms, reproduced from [28,30,31,33,37,53,54,76,86, 87,87–94].

- **Cosine curve.** The coordinates  $x$  and  $y$  of cosine curve are as:  $y = \frac{h}{2} \left( 1 - \cos \frac{\pi x}{L} \right)$ , where  $L$  and  $h$  are the span and apex height of the cosine curved beam.

### 3. Comparison of constant force/torque performances

To make the comparisons directly and clearly for the designers, an overview of achieved constant force/torque ranges of some existing CCFTMs in the last decade is presented in Fig. 12. The CCFTMs obtained by the aforementioned design method shows 1-DOF 1-stage constant force in a certain stroke after a certain preload region. In order not to be affected by out-of-plane width,

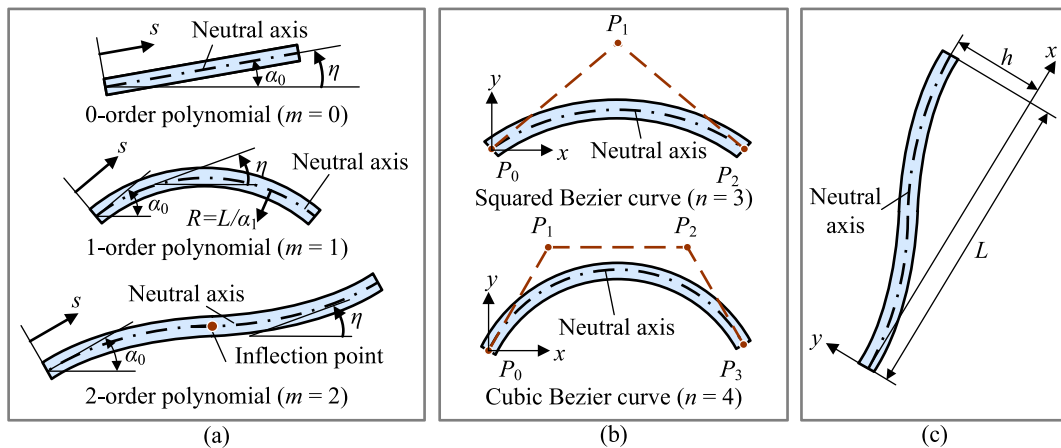


Fig. 11. Common curved beams with shape functions: (a) polynomial curve, reproduced from [31], (b) Bezier curve, reproduced from [28], and (c) Cosine curve, reproduced from [37].

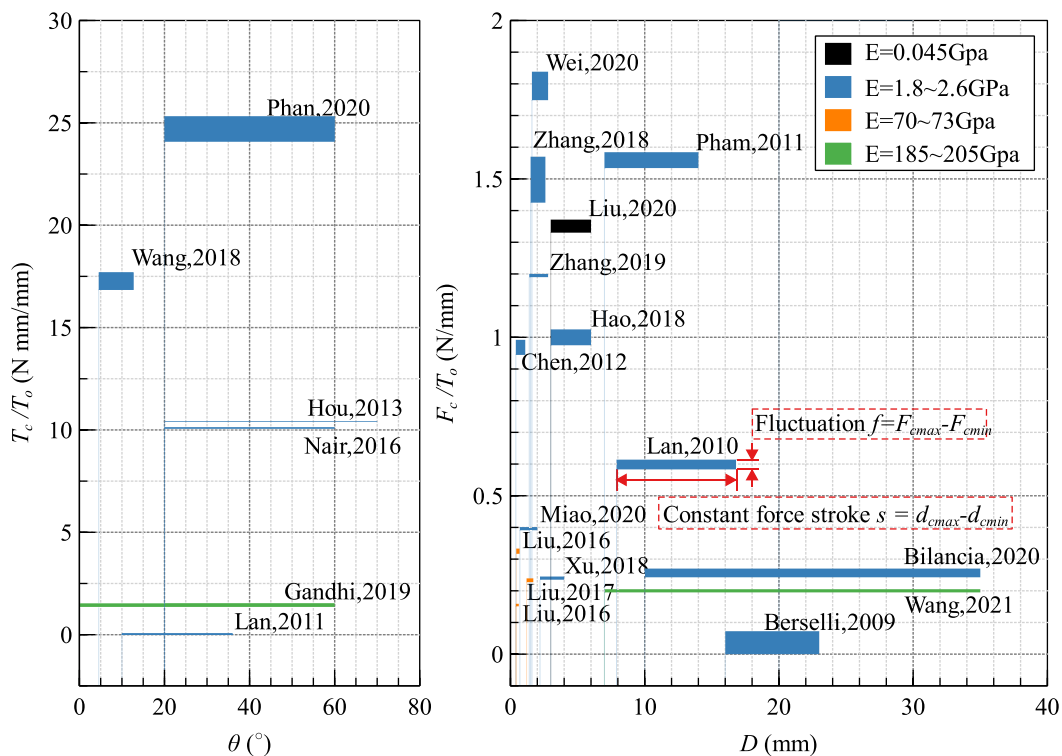


Fig. 12. An overview of achieved constant force/torque ranges of some existing compliant constant force/torque mechanisms in the last decade.

the constant forces and corresponding fluctuations per out-of-plane width are investigated in these works. In this section, we will provide a comparative view of the achieved force/torque ranges of existing 1-stage and multi-stages CCFTMs.

### 3.1. 1-stage compliant constant force/torque mechanisms

The constant force/torque values and stokes of 1-stage CCFTMs with their application fields are shown in Fig. 13. It can be observed that the field of micromanipulation is mainly occupied by Class BA and Class TB CCFMs, mainly including microgripping and microinjection, where the constant forces range in value from 0.62 N to 4.96 N within 0.4 ~ 4 mm. The piezoelectric stack and voice coil motor are commonly used as the actuators due to their high precision, large stiffness and fast response. In addition, the compliant amplification mechanisms are usually combined with the CCFMs serially to adapt to the situations that need larger

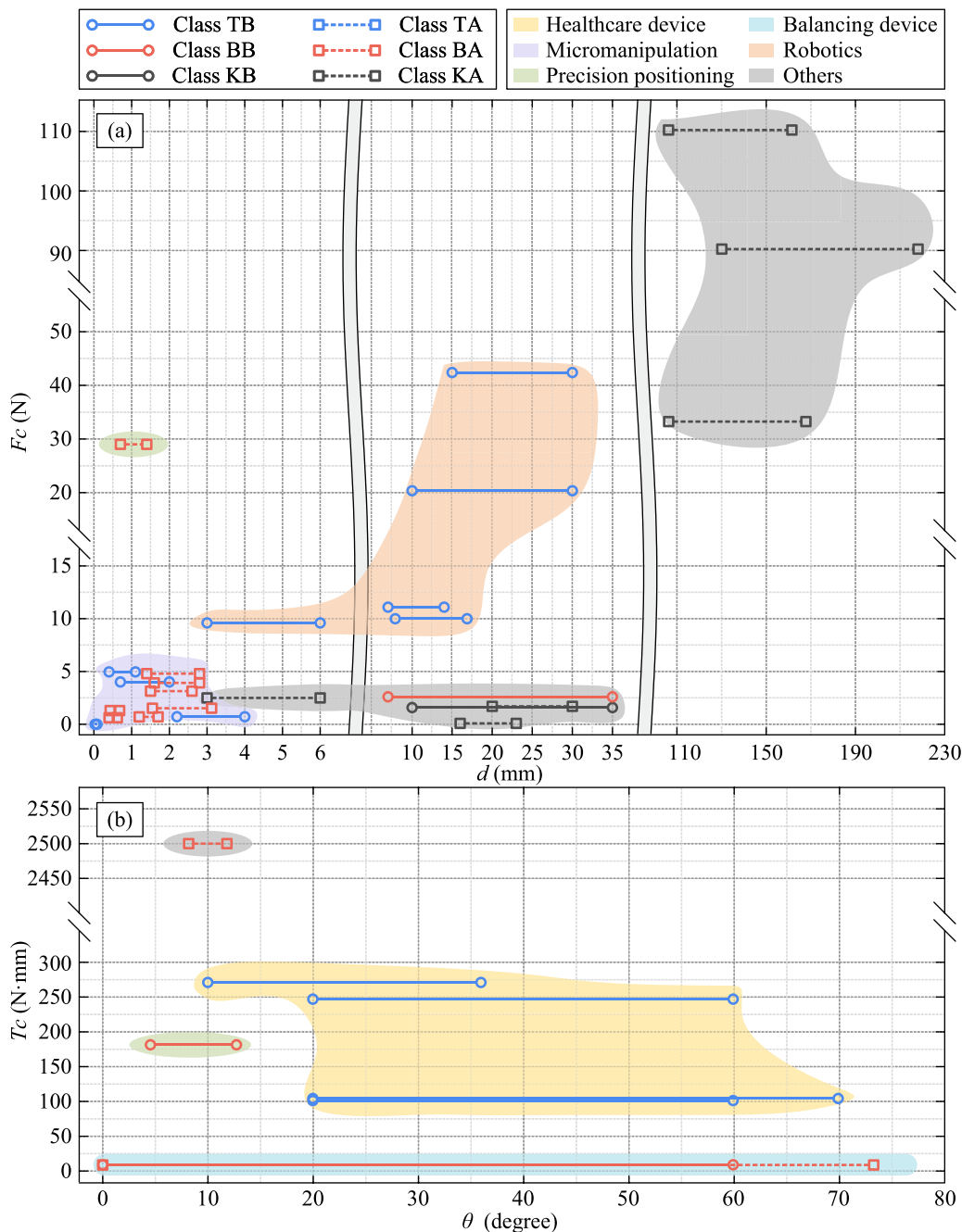


Fig. 13. Comparison of the constant force/torque values and strokes: (a) 1-stage compliant constant force mechanisms, and (b) 1-stage compliant constant torque mechanisms.

strokes or smaller output forces, such as bridge compliant amplification mechanism [70] and lever type compliant amplification mechanism [30]. As to the field of robotics, the CCFMs are usually applied for the adaptive robot end-effector operations, where the Class TB CCFMs are mainly concerned and their constant forces range in value from 9.6 N to 42.4 N within 3 ~ 30 mm. Some of them are mounted on two or more jaws [83,92]. Some Class TB CCTMs are utilized for surgical manipulations, such as rehabilitation devices [28,94], whose constant torques range in value from 101.3 N·mm to 271 N·mm within 10 ~ 70°. Besides, some Class BA and BB CCTMs are served as balancing devices that combine the merits of flexure joints and rigid joints, that is to say, they show zero stiffness and no energy storage without friction and gap [80].

In order not to be affected by structural parameters, the dimensionless constant forces/torques of CCFTMs with homogeneous flexure beams can be derived in Table 2. In this table, the dimensionless constant force/torque of these CCFTMs can be obtained



**Table 2**  
Normalization formulas for compliant constant force/torque mechanisms composed of homogeneous flexure beams.

Composition	Compliant constant force mechanisms with single beam	Compliant constant torque mechanisms with single beam	Compliant constant force mechanisms with multi beams
Diagram			
Formula	$F_{cn} = \frac{F_{ce} L_x^2}{EI}$	$T_{cn} = \frac{T_{ce} L_x}{EI}$	$F_{cn} = \frac{F_{ce} L_x^2}{EI}$

The compositions of compliant constant force/torque mechanisms in this table are described by their basic constant force/torque elements.

by using the following formula [31,96]:

$$\frac{F_{cn} L_{xn}^2}{EI_n} = \frac{F_{ce} L_x^2}{EI}, \frac{T_{cn} L_{xn}}{EI_n} = \frac{T_{ce} L_x}{EI}, \quad (1)$$

where  $F_c$  and  $T_c$  refer to constant force and torque; subscripts  $e$  denote the elemental ones;  $L_{xn}^2 / (EI_n) = 1$ ;  $E$  is the Young's modulus of used material;  $I = t_o t_i^3 / 12$  is the inertia moment of homogeneous flexure beam;  $t_o$  is the out-of-plane thickness;  $t_i$  is the in-plane thickness;  $L_x$  refers to the width of design domain in  $x$  direction; subscripts  $n$  denote the dimensionless counterparts.

Particularly, as to these CCFMs with their basic constant force elements composed of positive and negative stiffness beams, i.e. Class BA CCFMs, the transform of dimensionless constant force is realized by assuming their  $F - d$  curves are linear in the constant force strokes. The negative stiffness within constant force stroke of the inclined straight flexure beam with homogeneous sections ( $na$  type negative stiffness mechanism in Fig. 8(b)) can be simplified into an constant:  $-33EI/L^3$  [77]. Since the zero stiffness of constant force is obtained by the parallel combination of the negative stiffness and positive stiffness, their stiffness values can be regarded as opposite numbers in the constant force stroke. Therefore, the dimensionless formula is similar to one with single beam.

The comparison of the dimensionless constant force/torque values and strokes of CCFTMs with homogeneous flexure beams is shown in Fig. 14, where the basic constant force elements composed of rigid segments and flexure segments are not included since their kinetostatic performances are not only affected by the structural parameters of the flexure segments, resulting in difficulty to directly compare with the configurations as summarized in Table 2. Moreover, the safe factors of CCFTMs that are derived by dividing their yield strengths to the maximum stresses are also given in Fig. 15. Generally speaking, Class TB configurations are easier to obtain the CCFTMs with larger strokes and higher safety factors, which may because their basic constant force elements are mostly composed of the curved flexure beams with larger compliance than the straight beams in the same design domain. Similarly, Class BA-1- $pc//na$  configuration also shows the same characteristics compared with Class BA-1- $pa//na$ , since the effective length of  $pc$  type positive stiffness beam is longer than that of  $pa$  one.

### 3.2. Compliant constant force/torque mechanisms with multiple stages

As to the multi-DOF CCFM, one solution is to place a CCFM on each DOF [40,74]; the other one is to synthesize a spatial CCFM which can generate constant force in multiple directions [97]. As to the multi-stage CCFM, one is to make the constant force within a certain stroke linearly adjustable by adjusting the preload displacement [77,86,87]; the other is to synthesize the CCFM with different constant force values in several sub-strokes in a continuous total stroke [41,76]. The existing multi-stage CCFTMs generally based on stiffness combination. The first type CCFTMs can derive excellent adeptness, while has poor performance in switching continuity in a single travel. On the contrary, the other type ones have had only two constant force stages so far though better switching continuity.

## 4. Comparison of employed synthesis approaches

### 4.1. Overview of employed synthesis approaches

The classified configurations and virtual prototyping methods are over-viewed with high details in Table 3. This section will introduce the employed synthesis approaches, including the kinetostatic modeling methods and optimization algorithms applied.

#### 4.1.1. Rigid-body replacement approach

The Pseudo Rigid-Body method is widely used for kinetostatic modeling of compliant mechanisms, which is proposed in the 1990s [100]. The flexure beams or hinges are equivalent to the rigid rods and rigid pivots, which simplifies the modeling process greatly. On this basis, replacing the rigid joints of rigid-body constant force mechanisms by the appropriate flexure joints, RBRA is the most common synthesis approach for CCFTMs using kinematic limb-singularity, because the researches about those composed of

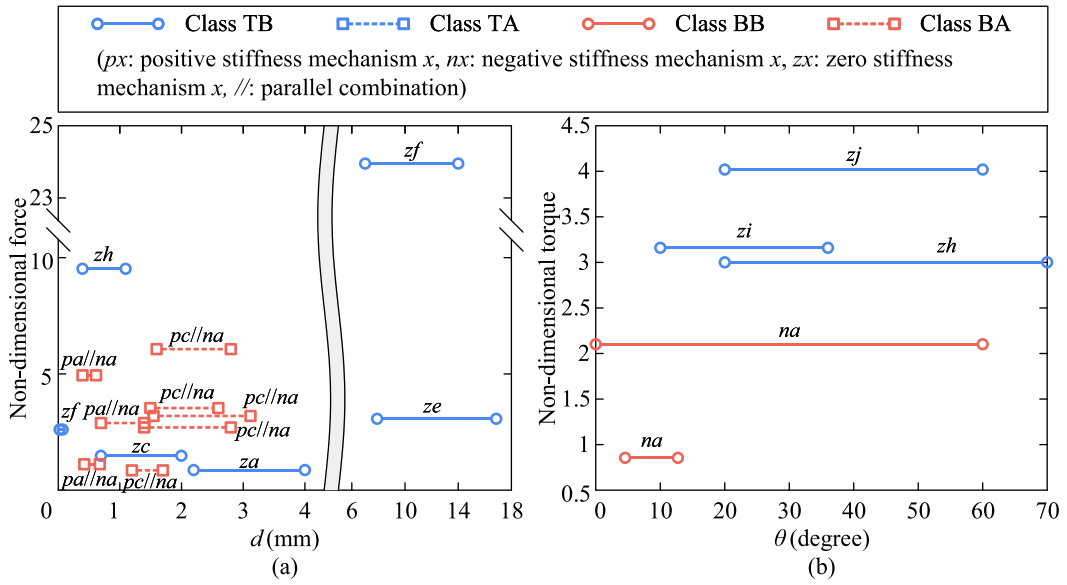


Fig. 14. Comparison of the dimensionless constant force/torque values and strokes: (a) 1-stage compliant constant force mechanisms with homogeneous flexure beams, and (b) 1-stage compliant constant force mechanisms with homogeneous flexure beams.

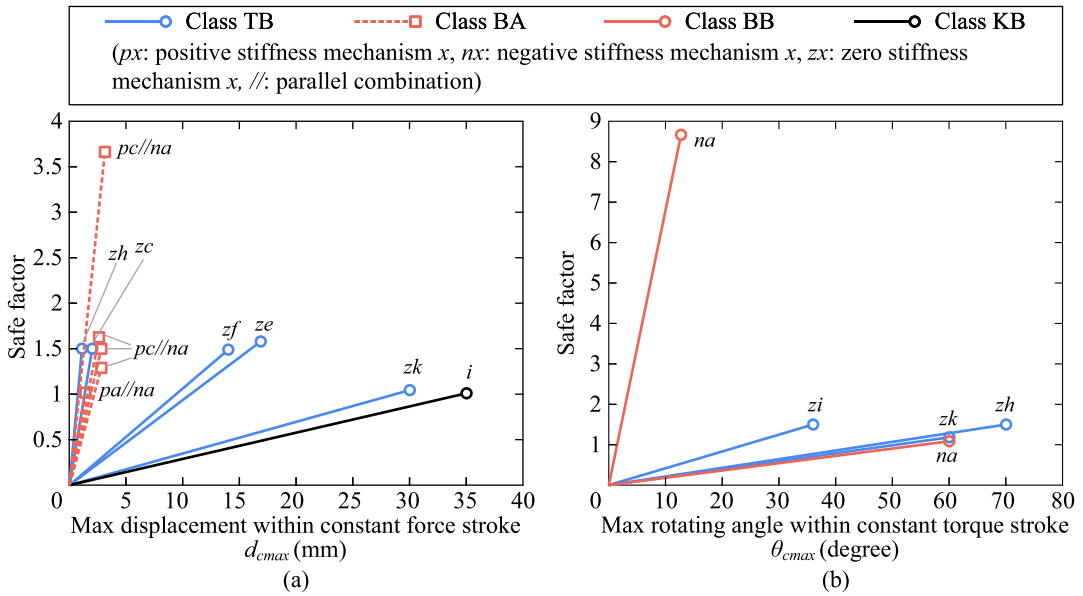


Fig. 15. Comparison of the safe factors versus their max displacement within constant force/torque stroke: (a) 1-stage compliant constant force mechanisms, and (b) 1-stage compliant constant torque mechanisms.

rigid mechanisms have been relatively mature. For this problem, the force/torque can be obtained based on the principle of virtual work as:

$$F = \frac{dU}{dd}, T = \frac{dU}{d\theta}, \tag{2}$$

where  $U$  denotes the potential energy.

As to optimization algorithm, Bilancia et al. proposed a special kind of complete CCFM based on crank–slider mechanism, using MATLAB Genetic Optimization Toolbox [48,49]. The basic constant force element is a long straight beam or a spline curved beam with continuous variable cross section, while the stress of the wider segment is close to zero in ANSYS software, i.e. the rigid-body segment.

Table 3

Literature overview of classified configurations and virtual prototyping method for synthesis of compliant constant force/torque mechanisms.

Configurations	Synthesis approach	Kinetostatic modeling method	Optimization algorithm
KA-1- <i>gc</i> ss[65], KA-1- <i>gd</i> ss[58], KA-1- <i>sss</i> [63,64], KA-1- <i>lpl</i> [47], KA-1- <i>ssl</i> [46], KA-1- <i>ssl</i> gc[39] KB-1- <i>i</i> [48,49]	Rigid-body replacement approach	Pseudo rigid-body method	
BA-1- <i>pa//na</i> [67–70], BA-1- <i>pc//na</i> [40,73,74,98], BB-1- <i>na</i> [78]	Rigid-body replacement approach Building block approach	Pseudo rigid-body method Elliptical integral method	Genetic algorithm
BA-1- <i>pc//na</i> [29] BA-2- <i>pa//na//na</i> [41], BA-2- <i>pe//na+na</i> '[71] BA-m-( <i>pd//pa</i> )'[77] BB-1- <i>na</i> [99]	Building block approach Building block approach Building block approach Building block approach	Elliptical integral method Elliptical integral method FEA Chained beam constraint method	Genetic algorithm Particle Swarm Optimization algorithm Gradient-based algorithm
TA-m-( <i>pf//nc</i> )'[86]	Topological Optimization approach	Generalized Shooting method	Global Optimization Toolbox Gradient-based algorithm
TB-1- <i>zb</i> [87]	Topological Optimization approach	Generalized Shooting method	Global Optimization Toolbox Gradient-based algorithm
TB-1- <i>ze</i> [31], TB-1- <i>zh</i> [38], TB-1- <i>zc</i> , TB-1- <i>zi</i> [28], TB-1- <i>zh</i> [33]	Topological Optimization approach	Generalized Shooting method	Genetic algorithm
TB-1- <i>zf</i> [37], TB-1- <i>zg</i> [76], TB-1- <i>zj</i> [94] TB-1- <i>zk</i> [54]	Topological Optimization approach Topological Optimization approach	FEA FEA	Global Optimization Toolbox Cuckoo Search algorithm
TB-1- <i>i</i> [81], TB-1- <i>ii</i> [83]	Topological Optimization approach	FEA	

#### 4.1.2. Topological optimization approach

TOA is the most common synthesis approach for CCFTMs using topological optimization, which can be divided into grid representation and geometry representation. As to grid representation, the basic constant force element obtained in this way is usually an irregular structure, which can be hardly solved by the aforementioned Pseudo-rigid-body method. Much attention has been attracted to the continuum topology optimization of the compliant mechanisms [84,85,101].

On this basis, the topology optimization using the Solid Isotropic Material with Penalization method and the size optimization using beam elements with ABAQUS software is proposed by Pedersen et al. which can be used to design compliant constant force mechanism which converts driving force into constant force output [102]. The size optimization step is used to remove hinge-like artifacts from the topology solution. Liu et al. adopted the Bidirectional Evolutionary Structural Optimization method to obtain the topology of CCFM with the size optimization by the cuckoo search algorithm [81,82]. After 3 mm preloading, a constant force of 9.45  $N$  can be output in 3 mm stroke with the fluctuation is 3%. The Graph-based TOA is most applied with geometry representation. In this way, many nonstandard flexure beams with explicit functions can show constant force performance under certain size conditions after compression, including polynomial, spline curve, Bezier curve, etc. By the kinetostatic modeling based on Generalized Shooting method, Lan et al. employed MATLAB nonlinear multi-variable function *fmincon* to optimize the shape and the size of three section composite flexible beams with their shape function as polynomial [31]. The similar method is also applied to optimize the single Bezier curve beam [28], and the multi section composite beams with arc and straight line [33,38]. The Non-dominated Sorting Genetic algorithm can also be used to optimize multi segment Bezier curve beams based on ABAQUS software, which is efficient due to the simplification from multiple targets into a virtual fitness function with non-dominated sorting procedure [37,53,76]. Based on the Chain Beam Constraint method, the Particle Swarm Optimization algorithm can be adopted to design straight beams with cross combinations. This is simple and easy to implement without multiple parameter adjustment. The Global Optimization Toolbox of MATLAB can also be used to optimize above nonstandard beams [92,94]. In particular, it can be used for interpolation optimization of curve beams with variable cross-sections. Rahman et al. formed the spline curve beams with variable cross-sections by interpolating variable diameter circles based on ANSYS software [42,54,93].

#### 4.1.3. Building block approach

Combining a number of known available building blocks, BBA have been used for synthesizing the CCFTMs using beam buckling theory. The building blocks are given in Fig. 8. As shown before, the basic constant force elements are usually composed of standard flexure beams, whose kinetostatic modeling is generally conducted by the Elliptic Integral method based on the Euler–Bernoulli beam theory. Since adopted in the 1980s, the Elliptic Integral method based on Euler–Bernoulli beam theory has been a powerful mathematical tool for the kinetostatic modeling of flexible slender beams with large deformation [103–105]. Although the solution accuracy is very high, it can only be solved in a closed form, which always leads to the complexity of the modeling process, thus

**Table 4**  
Comparison of the commonly used basic beam theories.

Basic theory	Euler–Bernoulli beam theory	Timoshenko beam theory
Hypothesis	The initial section plane perpendicular to the neutral axis remains perpendicular to the neutral axis during deformation.	The original section perpendicular to the neutral plane remains flat after deformation.
Governing equation	$\frac{1}{\rho(X)} = \frac{M(X)}{EI(X)}$ , where $E$ is Young’s modulus, $M \nabla X \partial$ is the bending moment at coordinate $X$ before deformation, $I(X)$ is the section moment of inertia about $Z$ axis, and $P(X)$ is the radius of curvature of plane compliant beam at coordinate $X$ .	$q(X) = \frac{d^2}{dX^2} (EI \frac{d\varphi(X)}{dX})$ , $\frac{d\omega(X)}{dX} = \varphi - \frac{1}{\kappa AG} \frac{d}{dX} (I \frac{d\varphi}{dX})$ , where $q(x)$ is the load concentration, $\kappa$ is the shear constant, $A$ is the cross-sectional area of the beam, and $E$ and $G$ are the elastic modulus and shear modulus, respectively.
Methods	Elliptic Integral method [104,105], Generalized Shooting method [113]	Timoshenko Beam Constraint method [110], Chained Beam Constraint method [114]

it is rarely used in the parameter optimization. Many efforts were devoted to solve this problem. The improvements of Pseudo-rigid-body method [106,107] and the simplifications of Elliptic Integral method [77] are carried out and proved to be effective. The Beam Constraint Model is proposed in 2006 [108]. It is mainly used in small deformation with deflection less than 10% of its dimension. The curvature is approximated by linearization, and the load is expressed by exact nonlinearity. Combined with the idea of chain algorithm [109], the chain beam constraint model based on the Timoshenko beam theory is established by solving each sub segment decomposed from the beam with Beam Constraint Model, which can be used in large deformation with deflection more than 10% [110,111]. Because the Timoshenko beam theory considers shear deformation and moment of inertia, and assumes that the original section perpendicular to the neutral plane remains plane after deformation, the accuracy of Chain Beam Constraint method is higher than that of Elliptic Integral method and SM in principle. The FEA softwares [112], such as ANSYS and ABAQUS, are often used as batch solver and verification tool to investigate the force–displacement relationships. In addition, the CCFTMs synthesized by RBRA and TOA can also be added in the building block library. With that, various configurations and corresponding building blocks can be fastly selected and virtually prototyped.

4.2. Comparison of kinetostatic modeling methods

4.2.1. Basic beam theories

The Euler–Bernoulli beam theory and Timoshenko beam theory are the commonly used basic beam theories to solve the kinetostatic models of flexure beams with large deformation, whose comparison are listed in Table 4. They can both be regarded as modeling bases [110]. The former ignores the shear deformation and moment of inertia, that is, it assumes that the section plane is always perpendicular to the neutral axis. On this basis, the shear deformation and moment of inertia are added to obtain Timoshenko beam theory. Although the initial section perpendicular to the neutral axis is no longer vertical after deformation, it is still assumed that the section is always planar during deformation.

4.2.2. Kinetostatic modeling methods

**Pseudo-rigid-body method.** Taking the double slider mechanism as an example, Fig. 16(a) shows the kinetostatic pseudo rigid-body models and motion trajectories. It can be seen that the pseudo rigid-body equivalent is similar to the inverse process of rigid-body replacement, which is represented by pseudo rigid bars, pseudo rigid hinges with torsion spring and pseudo rigid linear springs. The elastic potential energy of the pseudo rigid-body model can be derived as

$$U = \sum_{m=1}^M \frac{1}{2} k_{Rm} (\Delta\theta_m)^2 + \sum_{n=1}^N \frac{1}{2} k_{Pn} (\Delta s_n)^2 \tag{3}$$

where  $M$  and  $N$  are the quantities of the torsion springs and the linear springs;  $k_{Rm}$  and  $k_{Pn}$  are the revolute stiffness and prismatic stiffness ( $m = 1 \sim M, n = 1 \sim N$ );  $\Delta\theta_m$  is the change of rotation angle of torsion spring;  $\Delta s_n$  is the change of position of linear spring.

For the convenience of expression, the displacement  $s_g$  is generalized, including the linear displacement  $s$  and angular displacement  $\theta$ , as well as the force  $F_g$ . The principle of virtual work is a practical method to construct the equation of force equilibrium without the need to determine the internal force between two connecting bars. On this basis, the following is true:

$$\sum_{i=1}^{M+N} \delta W_i = \sum_{i=1}^{M+N} \vec{F}_{gi} \delta \vec{s}_{gi} = 0 \tag{4}$$

where  $\delta W_i$  refers to the virtual work of the whole mechanism;  $\delta \vec{s}_{gi}$  refers to the virtual displacement vector.

Then, the generalized force  $F_g$  can be determined as

$$F_g = \frac{dU}{ds_g} \tag{5}$$

Thus, the relationship between the driving force/torque and the driving displacement are obtained, which can represent several nonlinear stiffness characteristics. Among them, the constant force (zero stiffness) characteristic will appear once the stiffness of

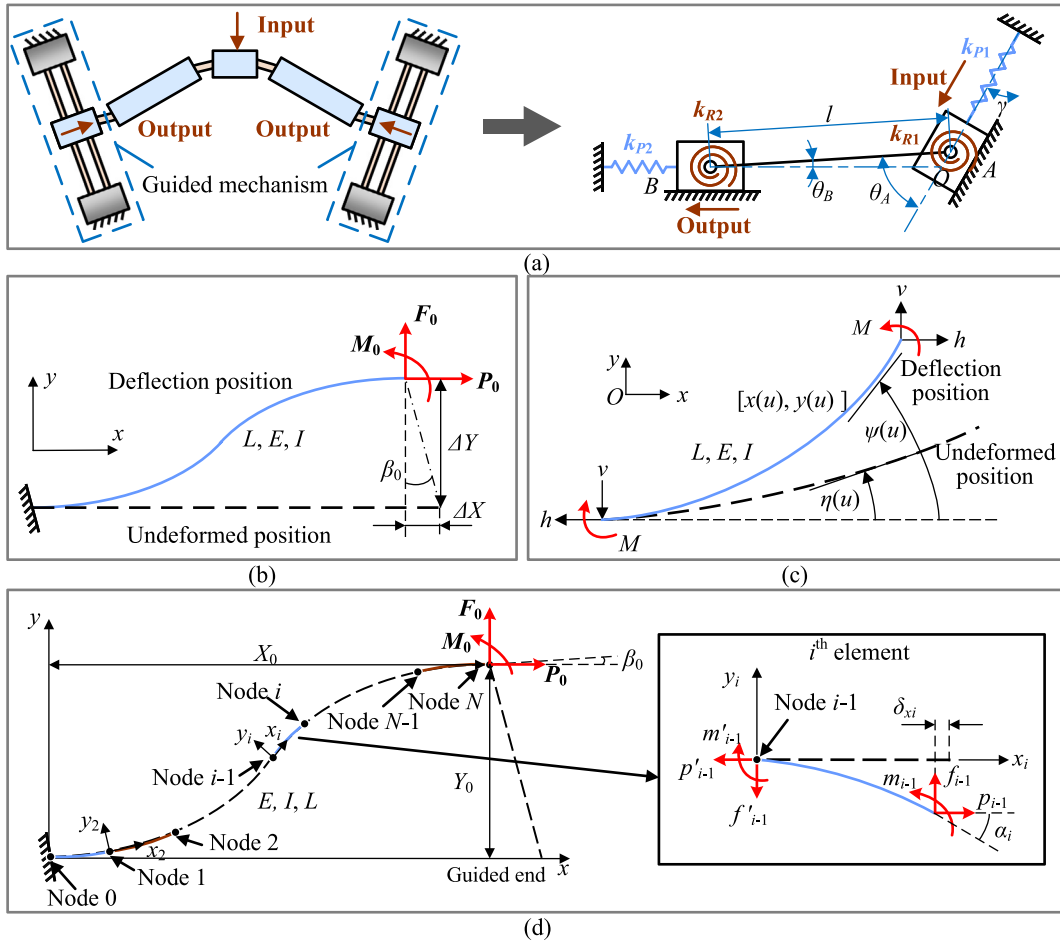


Fig. 16. Kinetostatic modeling methods for compliant constant force/torque mechanisms: (a) the pseudo-rigid-body model of the compliant constant force mechanism based on double slider mechanism [58], (b) the elliptic integral model of the straight homogeneous flexure beam [104,105], (c) the generalized shooting model of the curved homogeneous flexure beam [113], and (d) the chained beam constraint model [114].

torsion springs and linear springs are just combined to be zero in a stroke. Afterwards, the appropriate structural parameters of the flexible joints need to be obtained according to the stiffness requirements. The detailed formulas of various flexible joints are summarized in Table 5 [7,115].

**Elliptic Integral method.** The Elliptic Integral method gives an accurate closed-form solution of the load-deflection relationship based on the Bernoulli-Euler equation, which loses sight of the shear deformation and axial tensile deformation of the beam. The diagram of the kinetostatic model of a negative stiffness block by the Elliptic Integral method is shown in Fig. 16(b). In this model,  $x$ ,  $y$  and  $\theta$  denote the horizontal coordinate, vertical coordinate, and rotational angle of a random point  $A$  on the beam;  $P$  is the force reaction on the guided end;  $\beta$  is the angle between  $P$  and the  $x$ -axis. Based on the Euler-Bernoulli equation, the moment at any given point can be expressed as

$$M(X) = EIY''(X) = M_0 + F_0(L + \Delta X - X) - P_0(\Delta Y - \Delta Y(X)) \tag{6}$$

where  $E$  is the elasticity modulus of the material;  $I$  is the inertia moment.

After a series of transformations, the first and second elliptic integral functions are introduced as

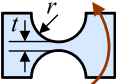
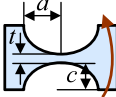
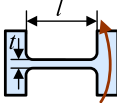
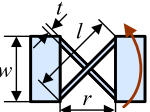
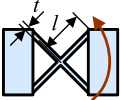
$$F(h, \varphi) = \int_0^\varphi \frac{d\delta}{\sqrt{1 - h^2 \sin^2 \delta}}$$

$$E(h, \varphi) = \int_0^\varphi \sqrt{1 - h^2 \sin^2 \delta} d\delta \tag{7}$$

where  $h$  is related to  $P$  and  $R$  that is generated by the derivative and integration of Eq. (6);  $\varphi$  is related to  $h$ ,  $\theta$  and  $\beta$ .

Then, the modeling values of the  $x$  and  $y$  coordinates of point  $A$  can be derived. Combined with the actual boundary conditions, the closed-form solution can be obtained by iterative search. The core of this method lies in the solution of critical buckling boundary

**Table 5**  
Stiffness formulas of the pseudo-rigid-body models of flexure hinges.

Type	Formula	Explanation
 Round notch hinge	$K = \frac{Ebt^3}{12rf}$	$f = \frac{(12s^2 + 8s + 2) \sqrt{4s + 1} + 12s(2s + 1)^2 \arctan \sqrt{4s + 1}}{(4s + 1)^{2.5} (2s + 1)},$ where $s = \frac{r}{t}$ ; $r$ is the radius of notch circle.
 Elliptical notch hinge	$K = \frac{Ebt^3}{12af}$	$f = \frac{(12s^2 + 8s + 2) \sqrt{4s + 1} + 12s(2s + 1)^2 \arctan \sqrt{4s + 1}}{(4s + 1)^{2.5} (2s + 1)},$ where $s = \frac{c}{t}$ ; $a$ and $c$ are the major and minor axes of notch ellipse.
 Short armed notch hinge	$K = \frac{Ebt^3}{12l}$	$l$ is the beam length.
 Cross reed hinge	$K = \frac{K_\theta Ebt^3}{24l}$	$K_\theta = 5.300 - 1.687n + 0.885n^2 = 0.209n^3 + 0.018n^4,$ where $n = \frac{r}{w}$ ; $r$ and $w$ are the effective length of flexible segment and the in-plane thickness of rigid segment.
 Wheel type hinge	$K = \frac{2Ebt^3}{3l}$	$l$ is the beam length.

$E$  is the Young's modulus of material;  $b$  is the out-of-plane thickness;  $t$  is the smallest in-plane thickness.

line and the judgment of buckling mode. Although it has a high accuracy, the derivation and implementation are quite intricate. Moreover, the iterative process may be sensitive to the initial guess of unknown parameters. In addition, some models also consider the effect of axial deformation [104].

**Generalized Shooting method.** The Shooting method is a numerical method for solving ordinary differential equations, which is suitable for the kinetostatic modeling of the curved beam with uniform section. The boundary value problem is transformed into the initial value problem. Taking polynomial curved beam as an example, Lan et al. adopted the Shooting method to derive its kinetostatic model based on the Euler–Bernoulli equations in Fig. 16(c) [31]. In this model,  $M$  denotes the bending moment at end of beam;  $\psi$  and  $\eta$  are the undeformed initial angle and the deformed end angle. The expression of bending moment is the same as Eq. (6). However, there are some small errors between modeling results and FEA simulation results with solid elements. On the one hand, this model based on the Euler–Bernoulli equations ignores the effects of shear and tensile deflection. On the other hand, the beam is assumed as a curved line on the neutral axis, thus ignoring the increase of the thickness at the connections between curved beams.

**Chain Beam Constraint method.** The Beam Constraint Model is proposed by Awtar et al. [108] to capture the close form solution of the flexible beams with small deflection (less than 10% of beam length) accurately, which can provide the parametric and close form expressions of load–deflection relations of the beam easily. The Chain Beam Constraint method divides a flexible beam into  $N$  elements, and each element is modeled by Beam Constraint Model. Thus, the Chain Beam Constraint method requires fewer elements than with the same desired accuracy. The diagram of kinetostatic model of the fixed-guided beam by Chain Beam Constraint method is shown in Fig. 16(d). In the model of the whole beam, node 0 represents the fixed end, and node  $N$  represents the guided end;  $F_0$ ,  $P_0$  and  $M_0$  denote the vertical component force, horizontal component force and moment applied at its guided end. In the model of the  $i$ th element  $1 \leq i \leq N$ , node  $i - 1$  is the coordinate origin;  $f_i$ ,  $p_i$  and  $m_i$  refer to the normalized vertical component load, horizontal component load, and moment;  $\delta x_i$ ,  $\delta y_i$  and  $\alpha_i$  refer to the normalized vertical component displacement, horizontal component displacement, and end slope, respectively. The normalized parameters are as

$$f_i = \frac{F_i L_i^2}{EI}, p_i = \frac{P_i L_i^2}{EI}, m_i = \frac{M_i L_i^2}{EI}, \delta x_i = \frac{U_{xi}}{L_i}, \delta y_i = \frac{U_{yi}}{L_i},$$

$$f_0 = \frac{F_0 L^2}{EI} = N^2 f_1, p_0 = \frac{P_0 L^2}{EI} = N^2 p_1, m_0 = \frac{M_0 L}{EI} = N m_N$$
(8)

where  $L_i$  is the length of  $i$ th element;  $E$  is the elasticity modulus of the material;  $I$  is the inertia moment.



**Table 6**  
Comparison of the commonly used kinetostatic modeling methods.

Models	Computing accuracy with large deformation	Computing efficiency	Axial deformation	Shear deformation
Pseudo-rigid-body model	low	High	Not considered	Not considered
Elliptic integral model	High	High	Not considered	Not considered
Elliptic integral model with axial deformation [104]	High	Middle	Considered	Not considered
Generalized shooting model [113]	High	High	Not considered	Not considered
Beam constraint model [108]	Middle	High	Considered	Not considered
Timoshenko beam constraint model [110]	Middle	High	Considered	Considered
Chained beam constraint model [114]	High	High	Considered	Considered
FEA	High	low	Considered	Considered

According to the kinetostatic models in [99,116], the load equilibrium equations of the  $i$ th element can be derived as

$$\begin{bmatrix} f'_{i-1} \\ p'_{i-1} \\ m'_{i-1} \end{bmatrix} = \begin{bmatrix} 1 & 0 & 0 \\ 0 & 1 & 0 \\ 1 + \delta x_i & -\delta y_i & 1 \end{bmatrix} \begin{bmatrix} f_i \\ p_i \\ m_i \end{bmatrix} \quad (9)$$

**Finite Element method.** FEA commercial softwares, including ANSYS and ABAQUS, have many advantages in optimization design and is therefore widely used [37,42,48,49,53,54,76,93,94]. The variables with initial values are taken as the structural parameters for FEA simulation to obtain kinetostatic performance that is delivered to the iterative process for optimal design. The parameters are continuously updated until the optimization objectives are achieved. Although the computational efficiency is relatively low, there is no faster and more accurate method for topology optimization with grid representation.

#### 4.2.3. Comparison of the kinetostatic modeling methods

As shown in Table 6, the computing accuracy and efficiency are compared as well as the consideration of axial and shear deformation. For more intuitive comparison, these methods are applied to  $na$  inclined straight homogeneous beams ( $E = 1.379$  GPa). Their  $F - d$  curves are shown in Fig. 17. It can be seen that the elliptical integral model considering axial deformation based on Euler–Bernoulli beam theory [104] is most similar to that of nonlinear FEA on the whole, while with the lowest computing efficiency except FEA due to search iterations. As to the chained beam constraint models based on Timoshenko beam theory, the chained beam constraint model with three elements ( $N=3$ ) [114] has almostly the same accuracy with the elliptical integral model considering axial deformation and better than that with two elements ( $N=2$ ) [116]. Additionally, the computing codes of chained beam constraint models with MATLAB are provided in the references.

### 4.3. Optimization methods and optimization algorithms

#### 4.3.1. Topological optimization methods

The continuum topology optimization with grid representation is widely used in the synthesis of compliant mechanisms, which includes the genetic algorithm-based topology optimization, Solid Isotropic Material Penalization method, Evolutionary Structural Optimization method, Homogenization, and so on [50,51]. Among them, the Solid Isotropic Material with Penalization method [102] and Bidirectional Evolutionary Structural Optimization method [81,82] have been employed in the synthesis of CCFTMs. Solid Isotropic Material with Penalization method is proposed by Sigmund et al. [117], which is a kind of Variable Density method. Each element in the design domain is given a relative density variable  $\mu$ , where  $\mu \in [0, 1]$ . The density  $\rho_{ei}$  of a random element  $i$  is

$$\rho_i = \mu \rho_0 \quad (10)$$

where  $\rho_0$  is the reference density of selected material.

Pedersen et al. predicted the load–deflection relation by Finite Element method with ABAQUS, and updated the value of  $\mu$  of each element until the minimum gap between output and objective force was minimized. If  $\mu = 0$ , the element is filled with “blank material” (white), i.e. void; If  $\mu = 1$ , the element is filled with solid material (black); if  $0 < \mu < 1$ , the physical properties of solid and blank materials can be obtained by the interpolation of penalty density function (gray). In addition, the value of  $\mu$  is generally not taken as 0 to avoid the singularity of the stiffness matrix. The gray element may be filled with solid or blank material. In order to avoid the uncertainty, the penalty factor  $p$  is introduced to calculate the stiffness matrix of gray element  $k_e$

$$k_e = \mu^p k_0 \quad (11)$$

where  $k_0$  is the stiffness matrix of black element.

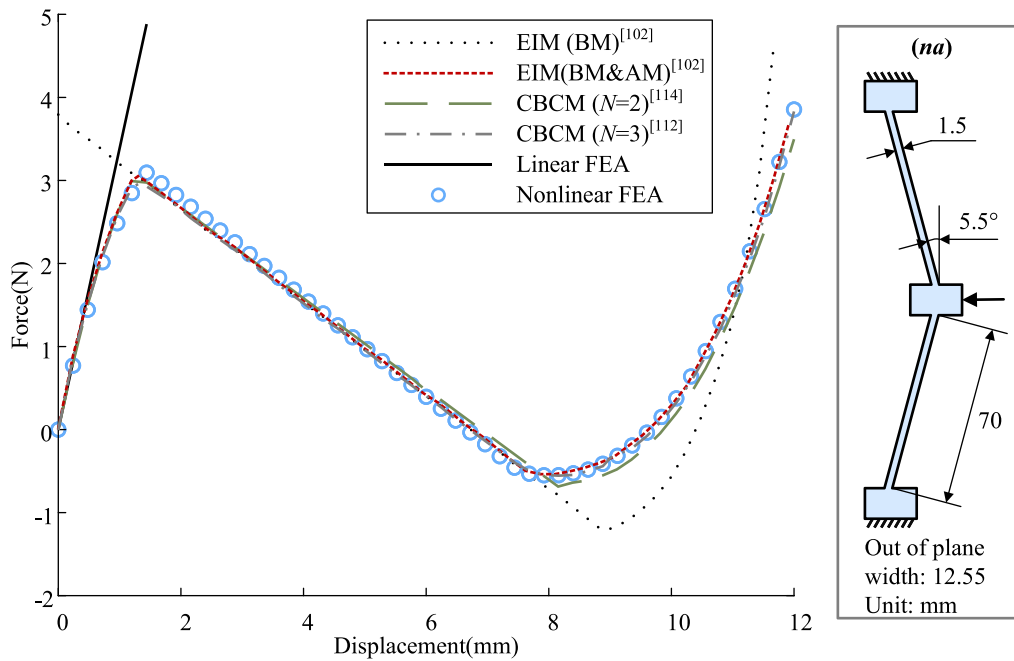


Fig. 17. Comparison of  $F-d$  curves of  $na$  type inclined straight homogeneous beams by various kinetostatic modeling methods.

Evolutionary Structural Optimization method is proposed by Xie et al. [118], which removes the inefficient elements step by step, and display the best force transfer path based on a certain optimization criteria. Bidirectional Evolutionary Structural Optimization is further proposed [119], which can add material while deletion. The high similarity between Bidirectional Evolutionary Structural Optimization and Solid Isotropic Material with Penalization method is present, while the relative density  $\mu$  of element in Bidirectional Evolutionary Structural Optimization is only 0 (blank material) and 1 (solid material). Obviously, the latter is more efficient since two tasks can be conducted simultaneously in one optimal cycle. Li et al. applied the batch mode of ANSYS to predict the load-deflection relation and optimize the topology with Bidirectional Evolutionary Structural Optimization. The optimal object is treated as an error minimization problem between output and objective forces.

The continuum topology optimization with geometry representation mainly includes the Level Set method, Moving Morphable Components-based method, Graph-based method, Material-mask method, and so on [85]. The Graph-based method is most frequently applied, where the curved beams with shape functions have been discussed above. In addition, the educational computing tools have been summarized in detail in Ref. [85].

#### 4.3.2. Optimization algorithms

The optimization algorithms can be divided into gradient-based algorithms and heuristic algorithms. The gradient is a vector composed of the partial derivatives of the objective function for each variable. The function grows fastest along the direction of the gradient and decreases fastest along the opposite direction of the gradient. Since the objective function and constraint function are not explicit functions of variables generally, it is difficult to solve the gradient. Therefore, some approximate methods are used. Lan et al. have done a lot of works, in which the gradient is approximated by finite difference method and realized by *fmincon* function of MATLAB Optimization Toolbox [28,31,33,38,86], which is a local optimization tool to find the minimum value. Liu et al. employed the adjoint method to approximate the gradient for the topology optimization by the method of Moving Asymptotes, which makes a series of subproblems with convexity and separable variables to approximate the nonlinear optimization problem [81,82]. Hence, the method of Moving Asymptotes may also be a feasible multi-parameter optimization algorithm.

The heuristic algorithms generally adopts stochastic iterative strategies, such as “genetic”, “crossover” and “mutation”, to screen according to objective function and constraint function, which narrows the solution space and makes an accurate local search. The Genetic Algorithm has been widely applied in multi-parameter optimization [48,49,92]. Most of them are implemented in MATLAB Global Optimization Toolbox. Moreover, there are some achievements in the optimization and variation of Genetic Algorithm. Pham, Wang, et al. employed the Genetic Algorithm with non-dominated sorting program to derive the load-deflection relation for better efficiency, which is realized by simplifying multiple objectives into a virtual fitness function [37,53,76,94]. The Particle Swarm Optimization Algorithm captures the optimal solution through the cooperation and information sharing among individuals in particle swarm without many parameters to adjust, which can be adopted to optimize the structural parameters of CCFM [99]. Each particle searches the optimal solution individually in the design domain, that is, individual extreme value, and shares it with other particles in the particle swarm. The optimal value of individual extreme value is regarded as the global optimal solution.

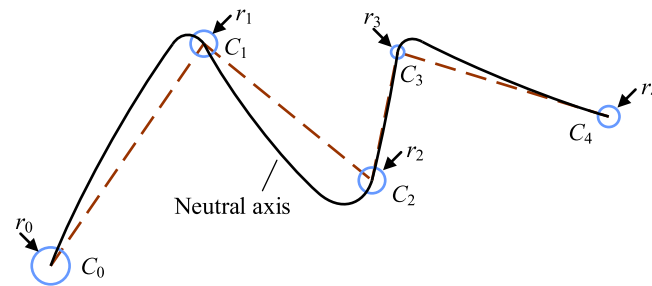


Fig. 18. Cubic spline interpolation with five different radius of the interpolation circles, reproduced from [93].

Different from the uniform section beam in all the above CCFMs, the interpolation optimization generate the flexible beams with variable section to generate constant force. So far, only cubic spline interpolation (see [42,54,93]) is an available case. The neutral axis of cubic spline curve based on the five interpolation points  $C_0$ ,  $C_1$ ,  $C_2$ ,  $C_3$  and  $C_4$  is shown in Fig. 18. The radius of each section perpendicular to the neutral axis at each interpolation point is not all the same value. The variation of section radius from one interpolation point to adjacent interpolation points is continuous, linear and monotonic. The synthesis of CCFM by interpolation optimization is realized by MATLAB Global Optimization Toolbox. Because this type curved beam has some rapidly changing angles, such as the angle at  $C_1$ , much attention should be paid to avoid the stress concentration caused by improper section radius.

## 5. Discussions

### 5.1. Rigid-body replacement approach

- **Merits.** The biggest advantage of RBRA is that the design process and kinetostatic analysis are both relatively simple, because the existing modeling methods of rigid-body mechanisms can be applied to the pseudo rigid-body models of compliant mechanisms equivalently.
- **Limitations.** Due to the kinematic singularity of the link-spring mechanism, the requirement of stiffness design is very strict when the revolute pairs are replaced by flexure hinges. Hence, the range and stroke of constant force are limited. Caused by the symmetrical arrangement and rigid segments, the size adaptability is also weakened. As to the kinetostatic modeling by Pseudo-rigid-body method, the cross section and shear deformation of the flexible segment are ignored, which leads to lower prediction accuracy, especially in the case of large deformation.
- **Applicability.** It is suitable for occasions with short design cycle, simple modeling, and low compliance requirements, as well as low demand for compactness and miniaturization, such as the rehabilitative constant torque device. Note that reasonable pseudo rigid-body modeling needs to ensure that the disadvantages brought by reducing the modeling accuracy are less than the benefits brought by model simplification.

### 5.2. Topological optimization approach

- **Merits.** The merits of synthesizing CCFTMs by the TOA are embodied in the following aspects: i) the optimal compact monolithic CCFTM can be obtained by the topology optimization; ii) the output force can be small enough for micro biomedical engineering owing to the larger compliance and no stiffness accumulation.
- **Limitations.** Although structural optimization is convenient to design from scratch and can get the optimal configuration, its limitations are reflected in the following aspects: i) due to the complexity of the shape, it is difficult to be fabricated by the reduced manufacturing, such as electrical discharge machining, while the additive manufacturing, such as 3D printing, still needs high precision requirements; ii) the result of optimization depends on mesh generation and quality; iii) the kinetostatic model is difficult to be parameterized and expressed analytically;
- **Applicability.** It is suitable for occasions with high requirements for constant force performances, compactness and miniaturization, while the design cycle is longer than RBRA and BBA. For example, it can be used in cell microinjection, where the constant force fluctuation needs to be very gentle, and the constant force value needs to be very small.

### 5.3. Building block approach

- **Merits.** The merits of the BBA are embodied in three aspects: i) the difficult problem is decomposed into several small problems to make the design simpler; ii) The modeling of the whole mechanism becomes simpler owing to the regular and simple shape of the building block; iii) the combination of building blocks with various stiffness curves may produce multi-stage constant force performance [41]. In addition, despite the positive stiffness block with large deflection, some scholars can capture the appropriate solution by Pseudo-rigid-body method because of its linear positive stiffness [67], which greatly simplifies the modeling process.

- **Limitations.** The parallel combination of the blocks will cause large stiffness before the constant force stroke, which is difficult to obtain a small enough constant force, such as for micro cell manipulation [30]. As to the kinetostatic modeling of the CCFTMs synthesized by BBA, the building blocks are usually modeled by relatively more complex methods due to the nonlinear bi-stable character of the negative stiffness block and large deflection, such as Elliptic Integral method and Chain Beam Constraint method. Although the solution accuracy is very high, the modeling process is much more complex than Pseudo-Rigid-Body method.
- **Applicability.** It is suitable for occasions with short design cycle, accurate modeling, and high compliance requirements, as well as high demand for compactness and miniaturization, such as the constant force microgripper for optical fiber assembly.

## 6. Challenges and future trends

In order to enable the interested researchers to more conveniently and systematically understand the synthesis methods and applicable scenarios of CCFTMs, this paper overviewed the recent advances, and summarized three synthesis methods, including RBRA, BBA and SOA. The related mechanism configurations, modeling methods, optimization methods and algorithms are introduced in detail.

Based on the related works above, it can be seen that the constant force performances, i.e. value, stroke, fluctuation, etc., of CCFTMs are not only determined by the design principle, modeling accuracy and optimization approach, but also severely affected by material properties and prototyping quality. To complete synthesis quickly with desired performances, the adaptive range, machinability, model simplification and fabricating quality need to be considered. These challenges for the synthesis of CCFMs are explained in detail as follows:

- **Limited adaptive range.** The adaptive range of common CCFTMs is limited due to the constant force of 1-DOF and 1-stage. In addition, the existing multi-stage CCFTMs highly rely on the adjustable devices, which increases the overall size and reduced the switching continuity. As to 2-stage CCFTMs, their design principles can be hardly employed to construct multi-stage ones due to the limitation of stroke.
- **Hard workability.** The traditional machining of compliant mechanism is a very difficult problem, because the large test error caused by insufficient machining accuracy occurs from time to time. Except for the CCFTMs composed of flexure hinges and standard beams, the CCFTMs with irregular structure or nonstandard beams are almost impossible to achieve the performances of the original design through traditional processing. Although additive manufacturing has great advantages for compliant mechanism manufacturing, the fatigue reliability of machining mechanism is usually questionable.
- **Modeling complexity.** The kinetostatic modeling for compliant mechanisms are usually more complicated than rigid mechanisms. Especially for the CCFTMs using topological optimization, the multiple iterative optimization process can be highly improved in efficiency with a proper balance between simplicity and accuracy.
- **Optimization methods and algorithms.** The topological optimization methods used for CCFTMs is still relatively a smaller quantity, especially for the grid representations. Besides, the optimization algorithms are heavily dependent on MATLAB's Toolboxes, while a lot of advanced optimization algorithms are not considered yet.

The focus of future researches is on the following aspects by inference.

- **Wider adaptive range.** The adaptive range of output force should be expanded in direction, value and multi-stage.
- **Better workability.** The shapes of CCFTMs should be as regular as possible to facilitate synthesis and fabrication. Better materials and manufacturing methods should be developed to reduce the experimental deviation and ensure the quality of processing high-volume consistency.
- **Simpler and faster modeling method.** Simpler and faster modeling methods should be proposed to simplify the modeling process and bring large convenience and higher efficiency.
- **Optimization methods and algorithms.** To deal with the mesh dependency and checkerboard patterns problems, more advanced topological optimization methods and algorithms should be further explored, such as the Bayesian optimization algorithm based on machine learning [120].

## Declaration of competing interest

The authors declare that they have no known competing financial interests or personal relationships that could have appeared to influence the work reported in this paper.

## Appendix. Abbreviations

- **CCFM:** Compliant constant force mechanism.
- **CCTM:** Compliant constant torque mechanism.
- **CCFTM:** Compliant constant force/torque mechanism.
- **F-d:** Force versus displacement.
- **RBRA:** Rigid-body replacement approach.

- **BBA:** Building block approach.
- **TOA:** Topological optimization approach.
- **FEA:** Finite Element Analysis.
- **Class XX-*n*:** CCFTMs using kinematic limb-singularity based on stiffness combination configurations.
- **Class KA:** CCFTMs using kinematic limb-singularity based on stiffness combination configurations.
- **Class KA-*n* – *x*:** see Fig. 5.
- **Class KB:** CCFTMs using kinematic limb-singularity based on direct zero stiffness configurations.
- **Class KB-*n* – *x*:** see Fig. 5.
- **Class BA:** CCFTMs using beam buckling theory based on stiffness combination configurations.
- **Class BA-*n* – *x*:** see Fig. 7.
- **Class BB:** CCFTMs using beam buckling theory based on direct zero stiffness configurations.
- **Class BB-*n* – *x*:** see Section 2.3.2.
- **Class TA:** CCFTMs using topological optimization based on stiffness combination configurations.
- **Class TA-*n* – *x*:** see Fig. 10.
- **Class TB:** CCFTMs using topological optimization based on direct zero stiffness configurations.
- **Class TB-*n* – *x*:** see Figs. 9 and 10.

## References

- [1] H. Huang, C. Dai, H. Shen, M. Gu, Y. Wang, J. Liu, L. Chen, L. Sun, Recent advances on the model, measurement technique, and application of single cell mechanics, *Int. J. Mol. Sci.* 21 (17) (2020) 6248, <http://dx.doi.org/10.3390/ijms21176248>.
- [2] J. Zhang, K. Lu, W. Chen, J. Jiang, W. Chen, Monolithically integrated two-axis microgripper for polarization maintaining in optical fiber assembly, *Rev. Sci. Instrum.* 86 (2) (2015) 025105, <http://dx.doi.org/10.1063/1.4907551>.
- [3] T.L. Thomas, K.V. Venkatasubramanian, G.K. Ananthasuresh, S. Misra, Surgical applications of compliant mechanisms: A review, *J. Mech. Robot.* 13 (2) (2021) 020801, <http://dx.doi.org/10.1115/1.4049491>.
- [4] H. Liu, J. Zhong, C. Lee, S.W. Lee, L. Lin, A comprehensive review on piezoelectric energy harvesting technology: Materials, mechanisms, and applications, *Appl. Phys. Rev.* 5 (4) (2018) 041306, <http://dx.doi.org/10.1063/1.5074184>.
- [5] L.L. Howell, Compliant mechanisms, in: J.M. McCarthy (Ed.), *21st Century Kinematics*, Springer London, London, 2013, pp. 189–216, [http://dx.doi.org/10.1007/978-1-4471-4510-3\\_7](http://dx.doi.org/10.1007/978-1-4471-4510-3_7).
- [6] W. Wright, O. Wright, The wright brothers' aeroplane, *Aeronaut. J.* 20 (79) (1916) 100–106, <http://dx.doi.org/10.1017/S2398187300142525>.
- [7] L.L. Howell, S.P. Magleby, B.M. Olsen, J. Wiley, *Handbook of Compliant Mechanisms*, Wiley Online Library, 2013, <http://dx.doi.org/10.1002/9781118516485>.
- [8] M. Verotti, A. Dochshanov, N.P. Belfiore, A comprehensive survey on microgrippers design: Mechanical structure, *J. Mech. Des.* 139 (6) (2017) 060801, <http://dx.doi.org/10.1115/1.4036351>.
- [9] S. Kirmse, L.F. Campanile, A. Hasse, Synthesis of compliant mechanisms with selective compliance – an advanced procedure, *Mech. Mach. Theory* 157 (2021) 104184, <http://dx.doi.org/10.1016/j.mechmachtheory.2020.104184>.
- [10] F. Wang, X. Zhao, Z. Huo, B. Shi, C. Liang, Y. Tian, D. Zhang, A 2-DOF nano-positioning scanner with novel compound decoupling-guiding mechanism, *Mech. Mach. Theory* 155 (2021) 104066, <http://dx.doi.org/10.1016/j.mechmachtheory.2020.104066>.
- [11] M. Ling, L.L. Howell, J. Cao, G. Chen, Kinestatic and dynamic modeling of flexure-based compliant mechanisms: a survey, *Appl. Mech. Rev.* 72 (3) (2020) 030802, <http://dx.doi.org/10.1115/1.4045679>.
- [12] M. Savia, H.N. Koivo, Contact micromanipulation - survey of strategies, *IEEE/ASME Trans. Mechatronics* 14 (4) (2009) 504–514, <http://dx.doi.org/10.1109/TMECH.2008.2011986>.
- [13] D.V. Sabarianand, P. Karthikeyan, T. Muthuramalingam, A review on control strategies for compensation of hysteresis and creep on piezoelectric actuators based micro systems, *Mech. Syst. Signal Process.* 140 (2020) 106634, <http://dx.doi.org/10.1016/j.ymsp.2020.106634>.
- [14] J. Ling, Z. Feng, D. Zheng, J. Yang, H. Yu, X. Xiao, Robust adaptive motion tracking of piezoelectric actuated stages using online neural-network-based sliding mode control, *Mech. Syst. Signal Process.* 150 (2021) 107235, <http://dx.doi.org/10.1016/j.ymsp.2020.107235>.
- [15] Z. Feng, J. Ling, M. Ming, W. Liang, K.K. Tan, X. Xiao, Signal-transformation-based repetitive control of spiral trajectory for piezoelectric nanopositioning stages, *IEEE/ASME Trans. Mechatronics* 25 (3) (2020) 1634–1645, <http://dx.doi.org/10.1109/TMECH.2020.2981966>.
- [16] M. Ming, W. Liang, Z. Feng, J. Ling, A.A. Mamun, X. Xiao, PID-type sliding mode-based adaptive motion control of a 2-DOF piezoelectric ultrasonic motor driven stage, *Mechatronics* 76 (2021) 102543, <http://dx.doi.org/10.1016/j.mechatronics.2021.102543>.
- [17] Y. Wei, Q. Xu, An overview of micro-force sensing techniques, *Sensors Actuators A* 234 (2015) 359–374, <http://dx.doi.org/10.1016/j.sna.2015.09.028>.
- [18] P. Wang, Q. Xu, Design and modeling of constant-force mechanisms: A survey, *Mech. Mach. Theory* 119 (2018) 1–21, <http://dx.doi.org/10.1016/j.mechmachtheory.2017.08.017>.
- [19] Q. Xu, Design and development of a novel compliant gripper with integrated position and grasping/interaction force sensing, *IEEE Trans. Autom. Sci. Eng.* 14 (3) (2015) 1415–1428, <http://dx.doi.org/10.1109/TASE.2015.2469108>.
- [20] Z. Nan, Q. Xu, Y. Zhang, W. Ge, Force-sensing robotic microinjection system for automated multi-cell injection with consistent quality, *IEEE Access* 7 (2019) 55543–55553, <http://dx.doi.org/10.1109/ACCESS.2019.2913592>.
- [21] W. Chen, J. Qu, W. Chen, J. Zhang, A compliant dual-axis gripper with integrated position and force sensing, *Mechatronics* 47 (2017) 105–115, <http://dx.doi.org/10.1016/j.mechatronics.2017.09.005>.
- [22] W. Jing, S. Chowdhury, M. Guix, J. Wang, Z. An, B.V. Johnson, D.J. Cappelleri, A microforce-sensing mobile microbot for automated micromanipulation tasks, *IEEE Trans. Autom. Sci. Eng.* 16 (2) (2018) 518–530, <http://dx.doi.org/10.1109/TASE.2018.2833810>.
- [23] Y. Wei, Q. Xu, A survey of force-assisted robotic cell microinjection technologies, *IEEE Trans. Autom. Sci. Eng.* 16 (2) (2018) 931–945, <http://dx.doi.org/10.1109/TASE.2018.2878867>.
- [24] C. Yang, Y. Xie, S. Liu, D. Sun, Force modeling, identification, and feedback control of robot-assisted needle insertion: a survey of the literature, *Sensors* 18 (2) (2018) 561, <http://dx.doi.org/10.3390/s18020561>.
- [25] K. Mauter, A. Hasse, How to prestress compliant mechanisms for a targeted stiffness adjustment, *Smart Mater. Struct.* 29 (8) (2020) 085021, <http://dx.doi.org/10.1088/1361-665X/ab9237>.
- [26] K.A. Tolman, E.G. Merriam, L.L. Howell, Compliant constant-force linear-motion mechanism, *Mech. Mach. Theory* 106 (2016) 68–79, <http://dx.doi.org/10.1016/j.mechmachtheory.2016.08.009>.

- [27] M.D. Murphy, A. Midha, L.L. Howell, Methodology for the design of compliant mechanisms employing type synthesis techniques with example, in: International Design Engineering Technical Conferences and Computers and Information in Engineering Conference, Vol. 12846, American Society of Mechanical Engineers, 1994, pp. 61–66, <http://dx.doi.org/10.1115/DETC1994-0179>.
- [28] C.C. Lan, J.Y. Wang, Design of adjustable constant-force forceps for robot-assisted surgical manipulation, in: 2011 IEEE International Conference on Robotics and Automation, 2011, pp. 386–391, <http://dx.doi.org/10.1109/ICRA.2011.5979556>.
- [29] Y. Wei, Q. Xu, Design and testing of a new force-sensing cell microinjector based on small-stiffness compliant mechanism, IEEE/ASME Trans. Mechatronics (2020) <http://dx.doi.org/10.1109/TMECH.2020.3003992>.
- [30] Q. Xu, Design and development of a flexure-based compact constant-force robotic gripper, in: Micromachines for Biological Micromanipulation, Springer, 2018, pp. 145–168, [http://dx.doi.org/10.1007/978-3-319-74621-0\\_7](http://dx.doi.org/10.1007/978-3-319-74621-0_7).
- [31] C.C. Lan, J.H. Wang, Y.H. Chen, A compliant constant-force mechanism for adaptive robot end-effector operations, in: 2010 IEEE International Conference on Robotics and Automation, 2010, pp. 2131–2136, <http://dx.doi.org/10.1109/ROBOT.2010.5509928>.
- [32] S.K. Agrawal, S.K. Banala, A. Fattah, V. Sangwan, V. Krishnamoorthy, J.P. Scholz, W.-L. Hsu, Assessment of motion of a swing leg and gait rehabilitation with a gravity balancing exoskeleton, IEEE Trans. Neural Syst. Rehabil. Eng. 15 (3) (2007) 410–420, <http://dx.doi.org/10.1109/TNSRE.2007.903930>.
- [33] C.W. Hou, C.C. Lan, Functional joint mechanisms with constant-torque outputs, Mech. Mach. Theory 62 (2013) 166–181, <http://dx.doi.org/10.1016/j.mechmachtheory.2012.12.002>.
- [34] V. Arakelian, S. Ghazaryan, Improvement of balancing accuracy of robotic systems: Application to leg orthosis for rehabilitation devices, Mech. Mach. Theory 43 (5) (2008) 565–575, <http://dx.doi.org/10.1016/j.mechmachtheory.2007.05.002>.
- [35] E.G. Merriam, K.A. Tolman, L.L. Howell, Integration of advanced stiffness-reduction techniques demonstrated in a 3D-printable joint, Mech. Mach. Theory 105 (2016) 260–271, <http://dx.doi.org/10.1016/j.mechmachtheory.2016.07.009>.
- [36] P. Bilancia, S.P. Smith, G. Berselli, S.P. Magleby, L.L. Howell, Zero torque compliant mechanisms employing pre-buckled beams, J. Mech. Des. 142 (11) (2020) 113301.
- [37] H.T. Pham, D.A. Wang, A constant-force bistable mechanism for force regulation and overload protection, Mech. Mach. Theory 46 (7) (2011) 899–909, <http://dx.doi.org/10.1016/j.mechmachtheory.2011.02.008>.
- [38] Y.H. Chen, C.C. Lan, Design of a constant-force snap-fit mechanism for minimal mating uncertainty, Mech. Mach. Theory 55 (2012) 34–50, <http://dx.doi.org/10.1016/j.mechmachtheory.2012.04.006>.
- [39] B. Li, G. Hao, On generating expected kinetostatic nonlinear stiffness characteristics by the kinematic limb-singularity of a crank-slider linkage with springs, Chin. J. Mech. Eng. 32 (1) (2019) 1–16, <http://dx.doi.org/10.1186/s10033-019-0369-z>.
- [40] X. Zhang, Q. Xu, Design and analysis of a 2-DOF compliant gripper with constant-force flexure mechanism, J. Micro-Bio Robot. 15 (1) (2019) 31–42, <http://dx.doi.org/10.1007/s12213-019-00112-4>.
- [41] T. Ye, J. Ling, X. Kang, Z. Feng, X. Xiao, A novel two-stage constant force compliant microgripper, J. Mech. Des. 143 (5) (2021) 053302, <http://dx.doi.org/10.1115/1.4048217>.
- [42] I. Gandhi, H. Zhou, Synthesizing constant torque compliant mechanisms using precompressed beams, J. Mech. Des. 141 (1) (2019) <http://dx.doi.org/10.1115/1.4041330>.
- [43] F. Ma, G. Chen, H. Wang, Large-stroke constant-force mechanisms utilizing second buckling mode of flexible beams: evaluation metrics and design approach, J. Mech. Des. 142 (10) (2020) 103303.
- [44] A. Midha, T.W. Norton, L.L. Howell, On the nomenclature, classification, and abstractions of compliant mechanisms, J. Mech. Des. 116 (1) (1994) 270–279, <http://dx.doi.org/10.1115/1.2919358>.
- [45] A. Midha, M.D. Murphy, L.L. Howell, Compliant constant-force mechanism and devices formed therewith, 1997, US Patent 5, 649, 454.
- [46] C. Boyle, L.L. Howell, S.P. Magleby, M.S. Evans, Dynamic modeling of compliant constant-force compression mechanisms, Mech. Mach. Theory 38 (12) (2003) 1469–1487, [http://dx.doi.org/10.1016/S0094-114X\(03\)00098-3](http://dx.doi.org/10.1016/S0094-114X(03)00098-3).
- [47] I.C. Ugwuoke, M.S. Abolarin, Design and development of class 2B-1pl compliant constant-force compression slider mechanism, Int. J. Eng. Manuf. (IJEM) 9 (3) (2019) 19–28, <http://dx.doi.org/10.5815/ijem.2019.03.02>.
- [48] P. Bilancia, A. Geraci, G. Berselli, On the design of a long-stroke beam-based compliant mechanism providing quasi-constant force, in: Smart Materials, Adaptive Structures and Intelligent Systems, Vol. 59131, American Society of Mechanical Engineers, 2019, [http://dx.doi.org/10.1115/SMASIS2019-5519\\_V001T03A001](http://dx.doi.org/10.1115/SMASIS2019-5519_V001T03A001).
- [49] P. Bilancia, G. Berselli, Design and testing of a monolithic compliant constant force mechanism, Smart Mater. Struct. 29 (4) (2020) 044001, <http://dx.doi.org/10.1088/1361-665X/ab6884>.
- [50] J.A. Gallego, J. Herder, Synthesis methods in compliant mechanisms: An overview, in: International Design Engineering Technical Conferences and Computers and Information in Engineering Conference, Vol. 49040, 2009, pp. 193–214, <http://dx.doi.org/10.1115/DETC2009-86845>.
- [51] M.D. Murphy, A. Midha, L.L. Howell, The topological synthesis of compliant mechanisms, Mech. Mach. Theory 31 (2) (1996) 185–199, [http://dx.doi.org/10.1016/0094-114X\(95\)00055-4](http://dx.doi.org/10.1016/0094-114X(95)00055-4).
- [52] P. Bilancia, G. Berselli, An overview of procedures and tools for designing nonstandard beam-based compliant mechanisms, Comput. Aided Des. (2021) 103001, <http://dx.doi.org/10.1016/j.cad.2021.103001>.
- [53] D.-A. Wang, J.-H. Chen, H.-T. Pham, A constant-force bistable micromechanism, Sensors Actuators A 189 (2013) 481–487, <http://dx.doi.org/10.1016/j.sna.2012.10.042>.
- [54] H.N. Prakashah, H. Zhou, Synthesis of constant torque compliant mechanisms, J. Mech. Robot. 8 (6) (2016) <http://dx.doi.org/10.1115/1.4034885>.
- [55] B.L. Weight, Development and design of constant-force mechanisms, (Master's thesis), Brigham Young University-Provo, 2002.
- [56] M. Liu, J. Zhan, B. Zhu, X. Zhang, Topology optimization of flexure hinges with a prescribed compliance matrix based on the adaptive spring model and stress constraint, Precis. Eng. (2021) <http://dx.doi.org/10.1016/j.precisioneng.2021.05.012>.
- [57] M. Liu, J. Zhan, B. Zhu, X. Zhang, Topology optimization of compliant mechanism considering actual output displacement using adaptive output spring stiffness, Mech. Mach. Theory 146 (2020) 103728, <http://dx.doi.org/10.1016/j.mechmachtheory.2019.103728>.
- [58] B. Li, G. Hao, Kinetostatic nonlinear stiffness characteristic generation using the kinematic singularity of planar linkages, in: Kinematics-Analysis and Applications, IntechOpen, 2019, pp. 65–81, <http://dx.doi.org/10.5772/intechopen.85009>.
- [59] J.G. Jenuwine, A. Midha, Synthesis of single-input and multiple-output port mechanisms with springs for specified energy absorption, J. Mech. Des. 116 (3) (1994) 937–943, <http://dx.doi.org/10.1115/1.2919473>.
- [60] S. Amine, O. Mokhiamar, S. Caro, Classification of 3T1R parallel manipulators based on their wrench graph, J. Mech. Robot. 9 (1) (2017) 011003, <http://dx.doi.org/10.1115/1.4035188>.
- [61] A. Karimi, M.T. Masouleh, P. Cardou, Avoiding the singularities of 3-RPR parallel mechanisms via dimensional synthesis and self-reconfigurability, Mech. Mach. Theory 99 (2016) 189–206, <http://dx.doi.org/10.1016/j.mechmachtheory.2016.01.006>.
- [62] B.D. Jensen, L.L. Howell, Bistable configurations of compliant mechanisms modeled using four links and translational joints, J. Mech. Des. 126 (4) (2004) 657–666, <http://dx.doi.org/10.1115/1.1760776>.
- [63] G. Berselli, R. Vertechy, G. Vassura, V.P. Castelli, Design of a linear dielectric elastomer actuator of conical shape with quasi-constant available thrust, in: 2009 International Conference on Intelligent Engineering Systems, IEEE, 2009, pp. 89–94, <http://dx.doi.org/10.1109/INES.2009.4924743>.



- [64] G. Berselli, R. Vertechy, G. Vassura, V.P. Castelli, Design of a single-acting constant-force actuator based on dielectric elastomers, *J. Mech. Robot.* 1 (3) (2009) <http://dx.doi.org/10.1115/1.3147182>.
- [65] G. Hao, A framework of designing compliant mechanisms with nonlinear stiffness characteristics, *Microsyst. Technol.* 24 (4) (2018) 1795–1802, <http://dx.doi.org/10.1007/s00542-017-3538-y>.
- [66] M.M. Kashani, L.N. Lowes, A.J. Crewe, N.A. Alexander, Nonlinear fibre element modelling of RC bridge piers considering inelastic buckling of reinforcement, *Eng. Struct.* 116 (2016) 163–177, <http://dx.doi.org/10.1016/j.engstruct.2016.02.051>.
- [67] Y. Liu, Q. Xu, Design of a compliant constant force gripper mechanism based on buckled fixed-guided beam, in: 2016 International Conference on Manipulation, Automation and Robotics At Small Scales (MARSS), IEEE, 2016, pp. 1–6, <http://dx.doi.org/10.1109/MARSS.2016.7561731>.
- [68] Y. Liu, Q. Xu, Design and analysis of a micro-gripper with constant force mechanism, in: 2016 12th World Congress on Intelligent Control and Automation (WCICA), IEEE, 2016, pp. 2142–2147, <http://dx.doi.org/10.1109/WCICA.2016.7578303>.
- [69] P. Wang, Q. Xu, Design of a flexure-based constant-force XY precision positioning stage, *Mech. Mach. Theory* 108 (2017) 1–13, <http://dx.doi.org/10.1016/j.mechmachtheory.2016.10.007>.
- [70] Y. Liu, Y. Zhang, Q. Xu, Design and control of a novel compliant constant-force gripper based on buckled fixed-guided beams, *IEEE/ASME Trans. Mechatronics* 22 (1) (2016) 476–486, <http://dx.doi.org/10.1109/TMECH.2016.2614966>.
- [71] J. Hu, X. Chen, Optimized design of a micro-motion stage with zero stiffness, *Opt. Precis. Eng.* 26 (6) (2018) <http://dx.doi.org/10.3788/OPE.20182606.1430>.
- [72] Y. Liu, Q. Xu, Design of a 3D-printed polymeric compliant constant-force buffering gripping mechanism, in: 2017 IEEE International Conference on Robotics and Automation (ICRA), IEEE, 2017, pp. 6706–6711, <http://dx.doi.org/10.1109/ICRA.2017.7989793>.
- [73] X. Zhang, G. Wang, Q. Xu, Design, analysis and testing of a new compliant compound constant-force mechanism, in: *Actuators*, Vol. 7, (4) Multidisciplinary Digital Publishing Institute, 2018, p. 65, <http://dx.doi.org/10.3390/act7040065>.
- [74] X. Zhang, Q. Xu, Design and development of a new 3-DOF active-type constant-force compliant parallel stage, *Mech. Mach. Theory* 140 (2019) 654–665, <http://dx.doi.org/10.1016/j.mechmachtheory.2019.06.019>.
- [75] Q. Xu, New flexure parallel-kinematic micropositioning system with large workspace, *IEEE Trans. Robot.* 28 (2) (2011) 478–491, <http://dx.doi.org/10.1109/TRO.2011.2173853>.
- [76] D.A. Wang, J.H. Chen, H.T. Pham, A tristable compliant micromechanism with two serially connected bistable mechanisms, *Mech. Mach. Theory* 71 (2014) 27–39, <http://dx.doi.org/10.1016/j.mechmachtheory.2013.08.018>.
- [77] G. Hao, J. Mullins, K. Cronin, Simplified modelling and development of a bi-directionally adjustable constant-force compliant gripper, *Proc. Inst. Mech. Eng. C* 231 (11) (2017) 2110–2123, <http://dx.doi.org/10.1177/0954406216628557>.
- [78] P. Wang, S. Yang, Q. Xu, Design and optimization of a new compliant rotary positioning stage with constant output torque, *Int. J. Precis. Eng. Manuf.* 19 (12) (2018) 1843–1850, <http://dx.doi.org/10.1007/s12541-018-0213-x>.
- [79] F. Ma, G. Chen, H. Wang, Large-stroke constant-force mechanisms utilizing second bending mode of flexible beams: Evaluation metrics and design approach, in: *International Design Engineering Technical Conferences and Computers and Information in Engineering Conference*, Vol. 59230, American Society of Mechanical Engineers, 2019, <http://dx.doi.org/10.1115/DETC2019-97813>, V05AT07A014.
- [80] F.M. Morsch, J.L. Herder, Design of a generic zero stiffness compliant joint, in: *International Design Engineering Technical Conferences and Computers and Information in Engineering Conference*, Vol. 44106, 2010, pp. 427–435, <http://dx.doi.org/10.1115/DETC2010-28351>.
- [81] C. Liu, M. Hsu, T. Chen, Y. Chen, Optimal design of a compliant constant-force mechanism to deliver a nearly constant output force over a range of input displacements, *Soft Robot.* 7 (6) (2020) 758–769, <http://dx.doi.org/10.1089/soro.2019.0122>.
- [82] C.H. Liu, M.C. Hsu, T.L. Chen, Topology and geometry optimization for design of a 3D printed compliant constant-force mechanism, in: 2020 IEEE/ASME International Conference on Advanced Intelligent Mechatronics (AIM), 2020, pp. 553–558, <http://dx.doi.org/10.1109/AIM43001.2020.9158933>.
- [83] C.-H. Liu, F.-M. Chung, Y.-P. Ho, Topology optimization for design of a 3D-printed constant-force compliant finger, *IEEE/ASME Trans. Mechatronics* (2021) <http://dx.doi.org/10.1109/TMECH.2021.3077947>.
- [84] H.A. Eschenauer, N. Olhoff, Topology optimization of continuum structures: a review, *Appl. Mech. Rev.* 54 (4) (2001) 331–390, <http://dx.doi.org/10.1115/1.1388075>.
- [85] B. Zhu, X. Zhang, H. Zhang, J. Liang, H. Zang, H. Li, R. Wang, Design of compliant mechanisms using continuum topology optimization: A review, *Mech. Mach. Theory* 143 (2020) 103622, <http://dx.doi.org/10.1016/j.mechmachtheory.2019.103622>.
- [86] Y.H. Chen, C.C. Lan, An adjustable constant-force mechanism for adaptive end-effector operations, *J. Mech. Des.* 134 (3) (2012) 031005, <http://dx.doi.org/10.1115/1.4005865>.
- [87] J.Y. Wang, C.C. Lan, A constant-force compliant gripper for handling objects of various sizes, *J. Mech. Des.* 136 (7) (2014) 071008, <http://dx.doi.org/10.1115/1.4027285>.
- [88] Q.D. Truong, T.N.D. K., D.A. Wang, Design and characterization of a mouse trap based on a bistable mechanism, *Sensors Actuators A* 267 (2017) 360–375, <http://dx.doi.org/10.1016/j.sna.2017.10.040>.
- [89] N.D.K. Tran, D.A. Wang, Design of a crab-like bistable mechanism for nearly equal switching forces in forward and backward directions, *Mech. Mach. Theory* 115 (2017) 114–129, <http://dx.doi.org/10.1016/j.mechmachtheory.2017.05.005>.
- [90] H. Van Tran, T.H. Ngo, P.L. Chang, I.T. Chi, N.D.K. Tran, D.A. Wang, A threshold gyroscope based on a bistable mechanism, *Mechatronics* 63 (2019) 102280, <http://dx.doi.org/10.1016/j.mechatronics.2019.102280>.
- [91] I.T. Chi, T.H. Ngo, P.L. Chang, N.D.K. Tran, D.A. Wang, Design of a bistable mechanism with B-spline profiled beam for versatile switching forces, *Sensors Actuators A* 294 (2019) 173–184, <http://dx.doi.org/10.1016/j.sna.2019.05.028>.
- [92] Y. Miao, J. Zheng, Optimization design of compliant constant-force mechanism for apple picking actuator, *Comput. Electron. Agric.* 170 (2020) 105232, <http://dx.doi.org/10.1016/j.compag.2020.105232>.
- [93] M.U. Rahman, H. Zhou, Design of constant force compliant mechanisms, *Int. J. Eng. Res. Technol.* 3 (7) (2014) 14–19.
- [94] T.V. Phan, H.T. Pham, C.N. Truong, Design and analysis of a compliant constant-torque mechanism for rehabilitation devices, in: *Advanced Materials*, Springer, 2020, pp. 541–549, [http://dx.doi.org/10.1007/978-3-030-45120-2\\_44](http://dx.doi.org/10.1007/978-3-030-45120-2_44).
- [95] X. Liu, F. Lamarque, E. Doré, P. Pouille, Multistable wireless micro-actuator based on antagonistic pre-shaped double beams, *Smart Mater. Struct.* 24 (7) (2015) 075028, <http://dx.doi.org/10.1088/0964-1726/24/7/075028>.
- [96] G. Hao, X. Kong, A normalization-based approach to the mobility analysis of spatial compliant multi-beam modules, *Mech. Mach. Theory* 59 (2013) 1–19, <http://dx.doi.org/10.1016/j.mechmachtheory.2012.08.013>.
- [97] Y.L. Kuo, C.C. Lan, A two-dimensional adjustable constant-force mechanism, *J. Mech. Des.* 142 (6) (2019) 063304, <http://dx.doi.org/10.1115/1.4044917>.
- [98] Y. Liu, D.J. Li, D. Yu, J. Miao, J. Yao, Design of a curved surface constant force mechanism, *Mech. Based Des. Struct. Mach.* 45 (2) (2017) 160–172, <http://dx.doi.org/10.1080/15397734.2016.1157692>.
- [99] N. Wang, J. Zhang, X. Zhang, Design of passive compliant constant-force mechanism, in: *Mechanism and Machine Science*, Springer, 2021, pp. 471–481, [http://dx.doi.org/10.1007/978-981-15-4477-4\\_33](http://dx.doi.org/10.1007/978-981-15-4477-4_33).
- [100] L.L. Howell, A. Midha, Parametric deflection approximations for end-loaded, large-deflection beams in compliant mechanisms, *J. Mech. Des.* 117 (1) (1995) 156–165, <http://dx.doi.org/10.1115/1.2826101>.

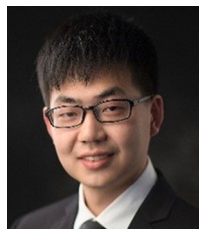
- [101] B. Niu, X. Liu, M. Wallin, E. Wadbro, Topology optimization of compliant mechanisms considering strain variance, *Struct. Multidiscip. Optim.* 62 (3) (2020) 1457–1471.
- [102] C.B.W. Pedersen, N.A. Fleck, G.K. Ananthasuresh, Design of a compliant mechanism to modify an actuator characteristic to deliver a constant output force, *J. Mech. Des.* 128 (5) (2006) 1101–1112, <http://dx.doi.org/10.1115/1.2218883>.
- [103] K. Mattiasson, Numerical results from large deflection beam and frame problems analysed by means of elliptic integrals, *Internat. J. Numer. Methods Engrg.* 17 (1) (1981) 145–153, <http://dx.doi.org/10.1002/nme.1620170113>.
- [104] G.L. Holst, G.H. Teichert, B.D. Jensen, Modeling and experiments of buckling modes and deflection of fixed-guided beams in compliant mechanisms, *J. Mech. Des.* 133 (5) (2011) <http://dx.doi.org/10.1115/1.4003922>.
- [105] A. Zhang, G. Chen, A comprehensive elliptic integral solution to the large deflection problems of thin beams in compliant mechanisms, *J. Mech. Robot.* 5 (2) (2013) <http://dx.doi.org/10.1115/1.4023558>.
- [106] H.J. Su, A pseudorigid-body 3R model for determining large deflection of cantilever beams subject to tip loads, *J. Mech. Robot.* 1 (2) (2009) <http://dx.doi.org/10.1115/1.3046148>.
- [107] Y.Q. Yu, S.K. Zhu, Q.P. Xu, P. Zhou, A novel model of large deflection beams with combined end loads in compliant mechanisms, *Precis. Eng.* 43 (2016) 395–405, <http://dx.doi.org/10.1016/j.precisioneng.2015.09.003>.
- [108] S. Awtar, S. Sen, A generalized constraint model for two-dimensional beam flexures: nonlinear load-displacement formulation, *J. Mech. Des.* 132 (8) (2010) 081008, <http://dx.doi.org/10.1115/1.4002005>.
- [109] T.C. Hill, A. Midha, A graphical, user-driven Newton-Raphson technique for use in the analysis and design of compliant mechanisms, *J. Mech. Des.* 112 (1) (1990) 123–130, <http://dx.doi.org/10.1115/1.2912569>.
- [110] G. Chen, F. Ma, Kinetostatic modeling of fully compliant bistable mechanisms using Timoshenko beam constraint model, *J. Mech. Des.* 137 (2) (2015) 022301, <http://dx.doi.org/10.1115/1.4029024>.
- [111] G. Chen, R. Bai, Modeling large spatial deflections of slender bisymmetric beams in compliant mechanisms using chained spatial-beam constraint model, *J. Mech. Robot.* 8 (4) (2016) <http://dx.doi.org/10.1115/1.4032632>.
- [112] H. Wang, X. Zhang, Input coupling analysis and optimal design of a 3-DOF compliant micro-positioning stage, *Mech. Mach. Theory* 43 (4) (2008) 400–410, <http://dx.doi.org/10.1016/j.mechmachtheory.2007.04.009>.
- [113] C.C. Lan, K.M. Lee, Generalized shooting method for analyzing compliant mechanisms with curved members, *J. Mech. Des.* 128 (4) (2005) 765–775, <http://dx.doi.org/10.1115/1.2202139>.
- [114] G. Chen, F. Ma, G. Hao, W. Zhu, Modeling large deflections of initially curved beams in compliant mechanisms using chained beam constraint model, *J. Mech. Robot.* 11 (1) (2019) 011002, <http://dx.doi.org/10.1115/1.4041585>.
- [115] L.L. Howell, *Compliant Mechanisms*, John Wiley, 2001, [http://dx.doi.org/10.1007/978-90-481-9751-4\\_302](http://dx.doi.org/10.1007/978-90-481-9751-4_302).
- [116] F. Ma, G. Chen, Modeling large planar deflections of flexible beams in compliant mechanisms using chained beam-constraint-model, *J. Mech. Robot.* 8 (2) (2016) 021018, <http://dx.doi.org/10.1115/1.4031028>.
- [117] M.P. Bendsoe, O. Sigmund, *Topology Optimization: Theory, Methods, and Applications*, Springer Science & Business Media, 2003.
- [118] Y.M. Xie, G.P. Steven, A simple evolutionary procedure for structural optimization, *Comput. Struct.* 49 (5) (1993) 885–896, [http://dx.doi.org/10.1016/0045-7949\(93\)90035-C](http://dx.doi.org/10.1016/0045-7949(93)90035-C).
- [119] O.M. Querin, G.P. Steven, Y.M. Xie, Evolutionary structural optimisation (ESO) using a bidirectional algorithm, *Eng. Comput.* 15 (8) (1998) 1031–1048, <http://dx.doi.org/10.1108/02644409810244129>.
- [120] N. Sultana, S.Z. Hossain, M. Abusaad, N. Alanbar, Y. Senan, S. Razzak, Prediction of biodiesel production from microalgal oil using Bayesian optimization algorithm-based machine learning approaches, *Fuel* 309 (2022) 122184, <http://dx.doi.org/10.1016/j.fuel.2021.122184>.



**Jie Ling** received his B.S. and Ph.D. degrees in Mechanical Engineering from School of Power and Mechanical Engineering, Wuhan University, China, in 2012 and 2018, respectively. From Aug. 2017 to Nov. 2017, he was a visiting Ph.D. student with Department of Automatic Control and Micro-Mechatronic Systems, FEMTO-st Institute, France. From Jan. 2019 to Jan. 2020, he was a Postdoctoral Research Fellow with Department of Biomedical Engineering, National University of Singapore, Singapore. Since Aug. 2020, he has been an Associate Research Fellow with College of Mechanical and Electrical Engineering, Nanjing University of Aeronautics and Astronautics, Nanjing, China. Dr. Ling's research interests include mechanical design and precision motion control of piezoelectric nanopositioning systems and micromanipulation robots.



**Tingting Ye** received her B.S. degree in Mechanical Engineering from School of Power and Mechanical Engineering, Wuhan University, Wuhan, China in 2019. Currently, she is a postgraduate student at School of Power and Mechanical Engineering, Wuhan University, Wuhan, China. Her research interests include compliant mechanism synthesis.



**Zhao Feng** received the B.S. and Ph. D. degrees in Mechanical Engineering from School of Power and Mechanical Engineering, Wuhan University, Wuhan, China in 2014 and 2020, respectively. From 2019 to 2020, he was also a visiting Ph. D. student at the Department of Electrical and Computer Engineering, National University of Singapore, Singapore. Currently, he is a Post-doctoral Fellow at the Faculty of Science and Technology, University of Macau, Macau, China. Dr. Feng's research interests include precision control, iterative learning control, nanopositioning and robotics.



**Yuchuan Zhu** received the Ph.D. degree in mechanical engineering from Nanjing University of Science and Technology, Nanjing, China in 2007. He joined the Nanjing University of Aeronautics and Astronautics, Nanjing, China in 2007, where he is currently a Full Professor with the Department of Mechanical and Electronic Engineering, College of Mechanical and Electrical Engineering. From 2014 to 2016, he was a Senior Visiting Scholar Fellow in the Department of Aeronautics and Astronautics, University of Maryland, USA. Dr. Zhu has published over 70 peer-reviewed papers in the areas of intelligent materials and structures, electro-hydraulic servo valves and electro-hydraulic actuators. His current research interests include intelligent materials and intelligent structures, advanced aviation hydraulics, electro-hydraulic servo valves and hydraulic simulation.



**Yangmin Li** received the B.S. and M.S. degrees in mechanical engineering from Jilin University, Changchun, China, in 1985 and 1988, respectively, and the Ph.D. degree in mechanical engineering from Tianjin University, Tianjin, China, in 1994. He is currently a Full Professor with the Department of Industrial and Systems Engineering, The Hong Kong Polytechnic University, Hong Kong. His research interests include micro/nanomanipulation, compliant mechanism, precision engineering, robotics, multibody dynamics and control. Dr. Li is an Associate Editor of the IEEE Transactions of Automation Science and Engineering, the Mechatronics, and the International Journal of Control, Automation, and Systems.



**Xiaohui Xiao** received the B.S. and M.S. degrees in Mechanical Engineering from Wuhan University, Wuhan, China, in 1991 and 1998, respectively, and the Ph.D. degree in mechanical engineering from Huazhong University of Science and Technology, Wuhan, China, in 2005. She joined the Wuhan University, Wuhan, China, in 1998, where she is currently a Full Professor with the Mechanical Engineering Department, School of Power and Mechanical Engineering. She has published over 30 papers in the areas of mobile robots, dynamics and control, sensors and signal processing. Her current research interests include mobile robotics, high-precision positioning control, and signal processing.